5-2018

Hybrid Flocking Control Algorithm with Application to Coordination between Multiple Fixed-wing Aircraft

Dawei Sun
Purdue University

HYBRID FLOCKING CONTROL ALGORITHM WITH APPLICATION TO COORDINATION BETWEEN MULTIPLE FIXED-WING AIRCRAFT

A Thesis

Submitted to the Faculty

of

Purdue University

by

Dawei Sun

In Partial Fulfillment of the

Requirements for the Degree

of

Master of Science in Aeronautics and Astronautics

May 2018

Purdue University

West Lafayette, Indiana

THE PURDUE UNIVERSITY GRADUATE SCHOOL
STATEMENT OF THESIS APPROVAL

Dr. Inseok Hwang, Chair

School of Aeronautics and Astronautics

Dr. Shaoshuai Mou

School of Aeronautics and Astronautics

Dr. Dengfeng Sun

School of Aeronautics and Astronautics

Approved by:

Dr. Weinong Chen

Head of the School Graduate Program

To my parents

ACKNOWLEDGMENTS

Foremost, I would like to express my deepest gratitude to my major advisor Prof. Inseok Hwang for his valuable guidance and constant support. Without his encouragement and suggestions, this thesis would not have been possible. Besides my major advisor, I would like to thank Prof. Shaoshuai Mou, Prof. Martin Corless and Prof. Dengfeng Sun for their time and advice on my research. In addition, I appreciate the support from my lab mates and friends. I would like to show my special gratitude to my senior mentor, Dr. Cheolhyeon Kwon. He has spent countless hours advising me on my research and my thesis composition. Last but not the least, I would like to thank my family members for their support and love.

TABLE OF CONTENTS

LIST OF TABLES

LIST OF FIGURES

ABSTRACT

M.S., Purdue University, May 2018. Hybrid Flocking Control Algorithm with Application to Coordination between Multiple Fixed-wing Aircraft. Major Professor: Inseok Hwang.

Flocking, as a collective behavior of a group, has been investigated in many areas, and in the recent decade, flocking algorithm design has gained a lot of attention due to its variety of potential applications. Although there are many applications exclusively related to fixed-wing aircraft, most of the theoretical works rarely consider these situations. The fixed-wing aircraft flocking is distinct from the general flocking problems by four practical concerns, which include the nonholonomic constraint, the limitation of speed, the collision avoidance and the efficient use of airspace. None of the existing works have addressed all these concerns. The major difficulty is to take into account the all four concerns simultaneously meanwhile having a relatively mild requirement on the initial states of aircraft. In this thesis, to solve the fixed-wing aircraft flocking problem, a supervisory decentralized control algorithm is proposed. The proposed control algorithm has a switching control structure, which basically includes three modes of control protocol and a state-dependent switching logic. Three modes of decentralized control protocol are designed based on the artificial potential field method, which helps to address the nonholonomic constraint, the limitation of speed and the collision avoidance for appropriate initial conditions. The switching logic is designed based on the invariance property induced by the control modes such that the desirable convergence properties of the flocking behavior and the efficient use of airspace are addressed. The proposed switching logic can avoid the fast mode switching, and the supervisor does not require to perform switchings frequently and

respond to the aircraft immediately, which means the desired properties can still be guaranteed with the presence of the dwell time in the supervisor.

1. INTRODUCTION

Flocking is commonly known as a collective motion of a group of interacting individuals with matched velocities [1]. With the growth of networked technology, a great amount of attention has been obtained by the flocking algorithm design due to a lot of potential applications, for instance, the formation flight for unmanned aerial systems [50] and for spacecraft [49]. The basic objective of a flocking algorithm is to induce certain collective behaviors, typically flocking centering, collision avoidance, and velocity matching, which are the three rules of flocking defined by Reynolds [7]. Different or additional objectives and constraints should be considered in some practical applications, for instance, the swarming of fixed-wing aircraft in the national airspace. Because of the larger range and longer endurance of fixed-wing aircraft, many flocking-related aerial applications are exclusively related to them. The multi-aircraft coordination in an air corridor with the service from the air traffic control system typically involves the fixed-wing aircraft flocking problem. Although there have been many developments for the general flocking algorithm design, none of the existing works have exhaustively addressed several concerns that are inherent in the fixed-wing aircraft applications. This prevent the general flocking algorithm from being applied directly.

At the early stage, most of the flocking-related works have primarily focused on the analysis of flocking behavior. References [1-7] are some representative examples of the early works. Reynolds in [7] has defined the flocking intuitively by introducing three characteristics that are flocking centering, collision avoidance, and velocity matching. Vicsek *et al.* in [6] have investigated the dynamic system of self-driven particles. Gazi and Passino in [3] have proved the stability of a type of flocking model theoretically. Tanner *et al.* in [4, 5], have proposed a stable flocking algorithm for fixed and dynamic communication graph topology. Later, to achieve the Reynolds rules and the obstacle

avoidance, Olfati-Saber has proposed a theoretical framework in [1] for the design of a flocking algorithm based on the continuous time consensus algorithm [20] and the artificial potential field method.

By extending the early works that have used the artificial potential field method, a lot of additional objectives have been addressed in later works. For instance, the connectivity preservation during formation or flocking has been addressed in [11-13, 19]; flocking in a bounded space has been considered in [8]; Olfati's work [1] has been extended in [10] such that the collective motion asymptotically converges to the virtual leader that has varying velocity. Besides the extensions of the artificial potential field method, some alternative approaches for flocking algorithm design have been investigated by later works, for example, some model predictive control schemes for multi-agent system problems proposed in [14-18], and the unified geometric projection approach proposed in [9]. It should be noted that the simple agent dynamics (*e.g.*, the single or double integrator model) without constraints is typically used in a range of flocking-related works, but for some applications related to fixed-wing aircraft flocking, more concerns and constraints should be addressed.

Compared with the general flocking algorithm, the flocking algorithm designed for fixed-wing aircraft should address four practical concerns. The nonholonomic constraint and the limitation of speed are the first two concerns. It is obvious that the fixed-wing aircraft is always approximately heading in the direction of the velocity vector, and unlike the automobile, the fixed-wing aircraft cannot fly backwards. The coincidence between the velocity vector and the orientation of the aircraft can be fulfilled by requiring that the heading of the velocity vector changes continuously over time. In addition, there are limitations on the minimum and the maximum speeds of fixed-wing aircraft in practical operations; in other words, the magnitude of the velocity vector should be bounded within a given interval. The safety issue is the third concern that must be addressed. In real-world applications, collision avoidance is a crucial objective. It should be noticed that the collision avoidance in practice can only be achieved conditionally because the control input is bounded. To gain better

applicability, less restrictive requirement is preferred. The fourth concern that should be addressed is the efficient use of airspace. Unlike ground robots, the motion of fixed-wing aircraft have an extra degree of freedom, so to take the advantage, the extra degree of freedom should be utilized to relax the condition for collision avoidance. On the other hand, considering the national airspace traffic regulation [53], it is preferred that the formation flights are adhering to the same altitude because the current Traffic Alert and Collision Avoidance System (TCAS) assists to resolve the conflict mainly by vertical separations [52]. Hence, the efficient use of airspace can be addressed by allowing the 3-dimensional motion to reach the consensus of altitude instead of restricting the motion in the 2-dimensional plane.

Even though there are some works considering the related situations, none of the works has theoretically rigorously addressed the aforementioned concerns. Currently, most of the works that consider the fixed-wing aircraft flocking, *e.g.*, [46-48], have only focused on the simulations and experiments rather than theoretical developments. Most of the general theoretical works on flocking (*e.g.*, [1, 3-5, 10-12]), as mentioned before, have only considered very simple agent dynamics, which is not enough to address the nonholonomic constraint and the other limitations. It is possible to transform the nonholonomic model to a simpler model via the feedback linearization technique, but there are usually some singularities for the coordinate transformation, which should be treated carefully. Although there have been works considering the nonholonomic model (*e.g.*, [23-37]), most of them have only focused on the applications for ground robots. These works do not care about the limitations of speed or the sharp heading changes, which are not acceptable for fixed-wing aircraft applications. The constant speed model is employed in [41-45, 51], whereas this assumption could cause difficulties to achieve self-separation or collision avoidance. For instance, the steering control has been considered in [51], but only the local convergence property has been theoretically verified. On the other hand, there are also some works that address the nonholonomic constraint, but the collision avoidance or the self-separation is not guaranteed explicitly (*e.g.*, [38-40]). In addition, the

efficient use of airspace has not been addressed in any flocking-related works so far. The existing works have considered either the 2-dimensional motion only [45] or the 3-dimensional motion without the consensus of altitude [41].

A control algorithm for fixed-wing aircraft flocking is proposed in this thesis such that the induced collective behavior is subject to the practical constraints: i) the nonholonomic constraint for aircraft dynamics; ii) the limitation on the horizontal speed of the aircraft; iii) the collision avoidance; and iv) the efficient use of airspace. To simultaneously address all these concerns, in general, requires a restrictive condition on the initial state (typically, the initial state should be included in a feasible subset of the state space), which is not desirable because it makes the applicability limited. To circumvent such a technical difficulty, a hybrid control idea is applied in this thesis. First, a set of modes of control protocol are designed such that the constraints are satisfied for the initial states in certain feasible sets, then an appropriate state-dependent switching logic is designed so that the overall feasible set for the initial state will be the union of the feasible set of each control mode. By doing so, a relatively mild requirement on the initial state can be obtained. The similar idea has appeared in some previous works. For instance, a multi-stage formation control strategy is proposed in [39] to address the nonholonomic constraint and the limitation of speed (but the collision avoidance and the efficient use of airspace are not considered in that work). In this thesis, more control objectives and constraints will be achieved by designing a supervisory decentralized control scheme. Following the aforementioned idea, three modes of decentralized control protocol are designed based on the artificial potential field method. It is assumed that the supervisor, or the monitoring system, can gather the state information from all aircraft and perform the state-dependent switching logic. With the invariance properties induced by the control modes, it can be shown that the fast mode switching can be avoided using the proposed switching logic, and the supervisor does not have to perform the switching logic frequently and respond to the aircraft immediately. In other words,

all desired properties can still be guaranteed even if the dwell time is implemented in the supervisor.

2. PRELIMINARIES

2.1 Notations

To avoid ambiguities, the notations are clarified in this section. $\mathbb{R}^+$ is used to denote the closed right real axis. $||*||_1$ and $||*||_2$ are used to denote the standard 1-norm and Euclidean norm in $\mathbb{R}^n$ respectively. $\mathcal{I}$ stands for the index set of agents when a multi-agent system is discussed. It is assumed that the cordiality of $\mathcal{I}$ is N, that is, the number of agents in the multi-agent system is N. $(*)_i$ is used to denote the state "$*$" of the i-th agent, and if the lower index i is omitted, we refer to the vector that collects this state from all agents. For instance, if v_i is used to denote the horizontal speed of the i-th agent, v is just a $\mathbb{R}^N$ vector defined as $[v_1, v_2, ..., v_N]^\mathsf{T}$.

2.2 σ-Norm

$||*||_\sigma$ is used to denote the σ-norm, which is a real valued function from $\mathbb{R}^n$ to $\mathbb{R}^+$ defined as

$$||s||_\sigma \triangleq \frac{1}{\epsilon}(\sqrt{1+\epsilon||s||_2{}^2}-1), \tag{2.1}$$

where ϵ is a positive constant. This function is used in [1] as a smoothed version of the Euclidean norm approximately such that the artificial potential field becomes smooth. This function is introduced here for the same purpose. Without causing confusion is caused, $||*||_\sigma$ will be used without specifying the dimension of the domain. The gradient of σ-norm can be computed as

$$\nabla||s||_\sigma = \frac{s}{\sqrt{1+\epsilon||s||_2{}^2}}, \tag{2.2}$$

which will be used several time during the derivation of the main result.

2.3 Invariance Principle

Invariance principle is commonly involved when the artificial potential method is considered (e.g. [1,10-13]). LaSalle's invariance principle, the standard invariance result, has been widely known. It is a powerful tool to prove the invariance and attractivity properties of a set in state space. It should be noticed that the standard result are for the autonomous system, and for general non-autonomous system, the invariance property cannot be easily guaranteed. However, for a special class of non-autonomous system, the asymptotically autonomous system, some extension of the invariance principle has been developed, which readers can refer to the Chapter VIII of [54] or Theorem 8.1 & 8.3 of [57]. In this work, the invariance principle for asymptotically autonomous system is used to prove some results.

2.4 Solutions of Switched Systems

For systems with switching dynamics, there are different concepts of solution. In this work, the switching logic of the controller is state-dependent and memoryless, so the overall dynamics can be treated as $\dot{x} = f(x)$ with piecewise continuous right-hand side. Since we will guarantee the fast switching is avoided, the solution in the sense of *Carathéodory* can be considered for simplicity. For a initial value problem with piecewise continuous dynamics, $\dot{x} = f(x)$, under the above assumption, a absolute continuous function $x(t)$ is said to be a solution in the sense of *Carathéodory* if it satisfies

$$x(t) = x(t_0) + \int_{t_0}^{t} f(x(\tau))d\tau. \tag{2.3}$$

With this concept of solution, the performance of the overall solution can be analyzed by considering the modes of control one-by-one. In the Chapter IV, three modes of control will be considered separately first and then construct the switching logic to get desired properties. When analyzing the modes of control separately, t_1, t_2 and t_3 are used to denote the initial time for the system with only mode 1, 2 and 3

respectively. Moreover, when discussing the overall trajectory induced by the hybrid control including all modes of control, t_0 is used to denote the overall initial time.

3. PROBLEM FORMULATION

3.1 Fixed-wing Aircraft Model

Let us consider the following second-order nonholonomic kinematic model for the dynamics of the i-th aircraft agent with the assumption that the behavior of the aircraft is not aggressive:

$$\begin{aligned} \dot{x}_i &= v_i \cos(\theta_i), \\ \dot{y}_i &= v_i \sin(\theta_i), \\ \dot{z}_i &= w_i, \\ \dot{v}_i &= a_i, \\ \dot{\theta}_i &= \phi_i, \\ \dot{w}_i &= \delta_i, \end{aligned} \tag{3.1}$$

where x_i, y_i are the horizontal coordinates for aircraft agent i and z_i stands for the attitude of aircraft agent i. v_i, w_i, θ_i are the horizontal component of velocity, vertical component of velocity and heading angle in the horizontal plane for agent i. a_i, w_i, and δ_i are respectively the horizontal acceleration, horizontal heading rate, and altitude rate, which are used for control inputs of aircraft. The assumption that the behavior of each agent is not aggressive means that w_i is small.

3.2 Control Objectives and Constraints

In addition to the velocity matching condition which is one of the general flocking objective, the major concerns of the fixed-wing aircraft flocking control can be mathematically described as the following objectives and constraints.

(O_1) Velocity Constraint: $\forall t \geq t_0, v_i \in [v_{min}, v_{max}]\ \forall i \in \mathcal{I}$;

(O_2) Collision Avoidance: $\forall t \geq t_0, d_{ij} \triangleq \sqrt{(x_i - x_j)^2 + (y_i - y_j)^2} + r|z_i - z_j| \geq d_{min}$ $\forall i, j \in \mathcal{I}$ with $i \neq j$, where r is a positive design parameter;

(O_3) State Consensus: As $t \to \infty$, $v_i \to \hat{v}$, $\theta_i \to \hat{\theta}$, $w_i \to 0$, $z_i \to 0$ $\forall i \in \mathcal{I}$;

(O_4) Self-Separation: As $t \to \infty$, $d_{ij} \geq \hat{d} \quad \forall i, j \in \mathcal{I}$ with $i \neq j$

(O_1) & (O_2) are constraints on the system state, and (O_3) & (O_4) are the desired properties for the flocking behavior. The nonholonomic and speed constraints are addressed by the objective (O_1) together with the aircraft kinematic model (3.1). The velocity matching from the Reynolds rules is interpreted as the objective (O_3). The efficient use of airspace is also covered by the objective (O_3) because we consider the 3-dimensional model and require the consensus of altitudes of agents. It is assumed that the vertical speed and altitude of each agent converge to zero without loss of generality. (O_4) is not explicitly corresponding to our major concerns, but it but is generally considered in many flocking problems for efficient and safe agent interactions [1].

The objective (O_2) is corresponding to the collision avoidance. Here a distance measurement other than the Euclidean norm in $\mathbb{R}^3$ is considered. Note that the definition of d_{ij} is inspired by the practical situation where the vertical distance between aircraft is less critical than the horizontal distance.

As the objectives imply, this work does not consider the flocking centering, one of the Reynolds rules. However, it would not be complicated to extend the control scheme proposed in this work to achieve the flocking centering. The theoretical framework proposed here is based on the artificial potential field method and the theory of switched control, which have been developed in many previous works. The possible extension of this work to achieve the flocking centering could be modifying the artificial potential field and/or adding new mode in the hybrid control scheme. For simplicity, let us not consider these extensions currently.

4. HYBRID FLOCKING ALGORITHM DESIGN

This section presents a supervisory decentralized control algorithm for fixed-wing aircraft flocking. Employing the hybrid system framework, the decentralized controller for each aircraft consists of three different modes of flocking control. Then, the mode switching is governed by the central supervisor based on the whole aircraft state information. Therefore, the state-dependent mode transition logic determines the overall flocking behavior of the aircraft such that control objectives and constraints (O_1)-(O_4) are achieved. Figure 1 illustrates the proposed hybrid control framework for fixed-wing aircraft flocking.

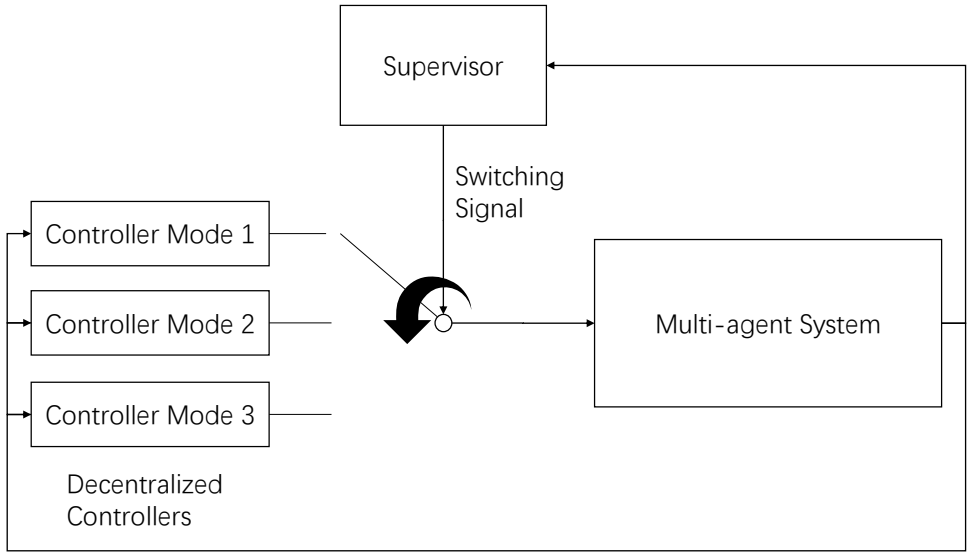

Fig. 4.1. State-Dependent Switching Control Scheme

Artificial potential field method is applied for designing each mode of the control protocol. As mentioned, this design technique has been wildly considered in related

works, *e.g.*, [1,10-13]. The basic idea of this technique is to treat each agent of the multi-agent system as a particle as well as a source of potential field. The motion of the agents is driven by the negative gradient of the integrated potential field, which is an analogue to the mechanical system in physics. By carefully designing the potential field, the desired behavior for the system can be guaranteed. The artificial potential field method is considered for control protocol design majorly based on two advantages. The first advantage is that the communication and computation load for each agent can be reduced by using finitely supported artificial potential field for each source, *i.e.*, each agent only need to react to its neighboring agents rather than all agents. The second advantage is that the artificial potential field method has desired scalability and is robust to agents failure.

In this thesis, the objectives related to constraints on the state, (O_1) and (O_2), will be achieved mainly by invariant set design. The invariance property will be induced by the artificial potential field method. By introducing appropriate artificial potential functions, each mode of control protocol can make some subsets of the state space invariant. The invariance property will not only be used to fulfill the constraints on the state but also be applied to design the switching logic. If the mode transition is determined by whether the multi-agent system state is in some invariant sets or not, the fast mode switching can be naturally excluded. In addition, the supervisor does not have to perform the switching logic too frequently or respond to aircraft immediately, and the objectives can still be guaranteed when the dwell time for performing the switching logic is introduced.

What follows is the detailed description of each of three flocking control modes, based on which the mode transition logic of the supervisor will be presented.

4.1 Mode 1: Heading Alignment & Vertical Separation

For this mode of the flocking control protocol, two main tasks are accomplished: heading alignment and vertical separation. The heading angle as well as the horizontal speed for each aircraft will be regulated with the constraint on the horizontal speed taken into account. Meanwhile, agents are separated vertically in order to gain distance for following stages.

The following definition is employed to the artificial potential field design for control mode 1.

Definition 4.1.1 *$\psi_1 : \mathbb{R}^+ \mapsto \mathbb{R}^+$ is a candidate artificial potential function for control mode 1 if it has the following properties: (i) it is a monotone decreasing function with continuous derivative; and (ii) it has a finite support, i.e., supp $\psi_1 = [0, \hat{d}_\sigma)$. The gradient of the candidate artificial potential function for control mode 1 is defined as*

$$f_1(\zeta) \triangleq \frac{d\psi_1(\eta)}{d\eta}|_{\eta=\zeta} \tag{4.1}$$

With the definition given above, for the i-th agent, the control mode 1 is given as

$$\begin{aligned} a_i &= -k_v(v_i - \hat{v}), \\ \phi_i &= -k_\theta(\theta_i - \hat{\theta}), \\ \delta_i &= -r\sum_{j\neq i} f_1(r||h_{ij}||_\sigma + ||p_{ij}||_\sigma)\hat{n}_{ij} - k_w w_i, \end{aligned} \tag{4.2}$$

where k_v, k_θ, k_w are positive constant, and $p_{ij} \triangleq [x_i - x_j, y_i - y_j]^\intercal \in \mathbb{R}^2$; $\hat{n}_{ij} \triangleq \frac{h_{ij}}{\sqrt{1+\epsilon||h_{ij}||_2{}^2}}$, where $h_{ij} \triangleq z_i - z_j$; f_1 is the gradient of a candidate artificial potential function for control mode 1. It should be noted that, by the fact that f_1 has a finite support, the computation of δ_i only depends on the neighboring agents of the $i-th$ agent, even if the sum is taken over all other agents in the expression.

The main properties for the flocking control mode 1 is summarized by the following theorem:

Theorem 4.1.1 *For the multi-agent system described by (3.1), the following statements are true if the control (4.2) is applied:*

(I) As $t \to \infty$, $v_i \to \hat{v}$, $\theta_i \to \hat{\theta}$ *and* $v_i(t) \in [v_{min}, v_{max}] \quad \forall t \geq 0, \quad \forall i \in \mathcal{I}$;

(II) $\forall t \geq t_1, d_{ij}(t) \geq d_{min}$ *for* $i, j \in \mathcal{I}$ *with* $i \neq j$ *if the following inequality is satisfied:*

$$\begin{aligned} ||p_{ij}(t_1)||_2 - \{\frac{1}{k_v}|v_i(t_1) - v_j(t_1)| + \frac{\hat{v}}{k_\theta}|\theta_i(t_1) - \theta_j(t_1)| \\ + \frac{1}{k_v k_\theta}(\frac{v_i(t_1) + v_j(t_1)}{2} - \hat{v})|\theta_i(t_1) - \theta_j(t_1)|\} \geq d_{min}; \end{aligned} \tag{4.3}$$

(III) As $t \to \infty$, $w_i \to 0$; *in addition, almost every configuration the system approaches has the property that* $d_{ij}^{\sigma} \triangleq r||h_{ij}||_\sigma + ||p_{ij}||_\sigma \geq \hat{d}_\sigma$ *between any two agents* $i \neq j$.

The first statement is corresponding to the heading alignment, velocity matching and the constraint on the horizontal speed. The second statement gives a sufficient condition on the initial state for collision avoidance. One can see that this condition mainly requires the mismatch between horizontal velocity vectors to be small, but it is independent to the mismatch between the initial headings and the desired heading. Note that the right-hand side of the inequality (4.3) is d_{min}, but if we restrict aircraft to move in the 2-D plane through all stages (vertical separations are not allowed), the right-hand side will need to be larger such that there are enough separations for later maneuvers. This explains how the extra degree of freedom during the transient stage can relax the requirement on the initial state. The proof of the first two statements of Theorem 4.1.1 is straightforward via algebra. The similar proof can be found in [41,42].

The third statement in the Theorem 4.1.1 claims the convergence of the multi-agent system state under the control mode 1. The interpretation of this statement is that the aircraft will gain enough separations for later maneuvers. The proof is based on the artificial potential field method and the invariance principle for the asymptotically autonomous system. The multi-agent system under the control mode 1 can be treated as two cascaded subsystems: the horizontal subsystem and the vertical

subsystem (see Figure 4.2). The part (I)&(II) of the Theorem 4.1.1 reveal the stability of the horizontal subsystem, then the vertical subsystem with the asymptotic input from the horizontal subsystem can be regarded as an asymptotically autonomous system. A Hamiltonian-like function is defined in order to show the convergence property. The detailed proof for the Theorem 4.1.1 is provided as below.

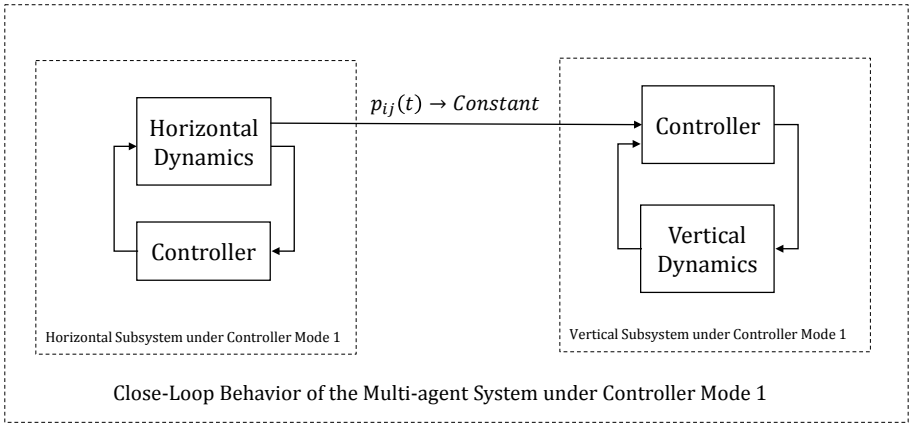

Fig. 4.2. Decoupling the Multi-agent System

Proof

The part (I) of the Theorem 4.1.1 can be directly seen from the equation (4.2). It is obvious that for any agent i, the following identity is true:

$$\begin{aligned} v_i(t) &= \hat{v} + (v_i(t_1) - \hat{v})e^{-k_v t}, \\ \theta_i(t) &= \hat{\theta} + (\theta_i(t_1) - \hat{\theta})e^{-k_\theta t}. \end{aligned} \tag{4.4}$$

To show the part (II) of the Theorem 4.1.1, first we show that $\forall i, j \in \mathcal{I}$ with $i \neq j$, $\frac{d}{dt}||p_{ij}||_2$ converges to zero exponentially fast. If $||p_{ij}||_2 \neq 0$, we have

$$\begin{aligned}
\frac{d}{dt}||p_{ij}||_2 &= \frac{1}{||p_{ij}||_2} p_{ij}^{\intercal} \dot{p}_{ij} \\
&\leq \frac{1}{||p_{ij}||_2} ||p_{ij}||_2 ||\dot{p}_{ij}||_2 \\
&= \sqrt{(v_i \sin(\theta_i) - v_j \sin(\theta_j))^2 + (v_i \cos(\theta_i) - v_j \cos(\theta_j))^2} \\
&= \sqrt{v_i^2 + v_j^2 - 2v_i v_j (\sin(\theta_i)\sin(\theta_j) + \cos(\theta_i)\cos(\theta_j))} \\
&= \sqrt{v_i^2 + v_j^2 - 2v_i v_j (\cos(\theta_i - \theta_j))} \\
&= \sqrt{(v_i - v_j)^2 + 2v_i v_j (1 - \cos(\theta_i - \theta_j))} \\
&= \sqrt{(v_i - v_j)^2 + 4v_i v_j \sin^2(\frac{\theta_i - \theta_j}{2})} \\
&\leq \sqrt{(v_i - v_j)^2 + 4v_i v_j (\frac{\theta_i - \theta_j}{2})^2}.
\end{aligned} \tag{4.5}$$

Recall that for an arbitrary $\mathbb{R}^2$ vector η, $||\eta||_2 \leq ||\eta||_1 \leq \sqrt{2}||\eta||_2$ holds, so if let $\eta = [v_i - v_j, \sqrt{v_i v_j}(\theta_i - \theta_j)]^{\intercal}$, we get

$$\begin{aligned}
\frac{d}{dt}||p_{ij}||_2 &\leq |v_i - v_j| + \sqrt{v_i v_j}|\theta_i - \theta_j| \\
&\leq |v_i - v_j| + \frac{v_i + v_j}{2}|\theta_i - \theta_j|.
\end{aligned} \tag{4.6}$$

Similarly,

$$\begin{aligned}
\frac{d}{dt}||p_{ij}||_2 &= \frac{1}{||p_{ij}||_2} p_{ij}^{\intercal} \dot{p}_{ij} \\
&\geq -\frac{1}{||p_{ij}||_2} ||p_{ij}||_2 ||\dot{p}_{ij}||_2 \\
&\geq -\sqrt{(v_i - v_j)^2 + 4v_i v_j (\frac{\theta_i - \theta_j}{2})^2} \\
&\geq -|v_i - v_j| - \frac{v_i + v_j}{2}|\theta_i - \theta_j|.
\end{aligned} \tag{4.7}$$

Together with (4.4), it is shown that $\frac{d}{dt}||p_{ij}||_2$ converges to zero exponentially fast. Now we can show (II) by contradiction. Assume there are two agents i and j that collide at t^*. By the continuity of $\frac{d}{dt}||p_{ij}(t)||_2$, we have

$$\begin{aligned}
d_{min} &> ||p_{ij}(t^*)||_2 \\
&= ||p_{ij}(0)||_2 + \int_0^{t^*} \frac{d}{dt}||p_{ij}(t)||_2 dt \\
&\geq ||p_{ij}(0)||_2 - \int_0^{t^*} |v_i - v_j| + \frac{v_i + v_j}{2}|\theta_i - \theta_j| dt \\
&\geq ||p_{ij}(0)||_2 - \int_0^{\infty} |v_i - v_j| + \frac{v_i + v_j}{2}|\theta_i - \theta_j| dt \\
&= ||p_{ij}(t_1)||_2 - \int_0^{\infty} \{|v_i(t_1) - v_j(t_1)|e^{-k_v t} \\
&\quad + [\hat{v}(1 - e^{-k_v t}) + \frac{v_i(t_1) + v_j(t_1)}{2} e^{-k_v t}]|\theta_i(t_1) - \theta_j(t_1)|e^{-k_\theta t}\} dt \\
&= ||p_{ij}(t_1)||_2 - \{\frac{1}{k_v}|v_i(t_1) - v_j(t_1)| \\
&\quad + \frac{\hat{v}}{k_\theta}|\theta_i(t_1) - \theta_j(t_1)| + \frac{1}{k_v k_\theta}(\frac{v_i(t_1) + v_j(t_1)}{2} - \hat{v})|\theta_i(t_1) - \theta_j(t_1)|\},
\end{aligned} \tag{4.8}$$

which is contradictory to (4.3). Therefore, if the initial condition satisfies (4.3), there will not be any collision, i.e., $\forall t \geq t_1, d_{ij}(t) \geq d_{min}\ \forall i, j \in \mathcal{I}$ with $i \neq j$.

The part (III) of the Theorem 4.1.1 can be shown by considering the following Lyapunov like function:

$$\begin{aligned}
H_1 &\triangleq PE_1(z, t) + KE_1(w) + G(t) \\
&\triangleq \frac{1}{2}\sum_{i \in \mathcal{I}} \sum_{j \neq i \in \mathcal{I}} \psi_1(r||h_{ij}||_\sigma + ||p_{ij}||_\sigma) + \frac{1}{2}\sum_{i \in \mathcal{I}} {w_i}^2 + G(t)
\end{aligned} \tag{4.9}$$

where $G(t)$ takes the form of $G(t) = Ae^{at}$ such that $\dot{G}(t) + \frac{1}{2}\sum_{i\in\mathcal{I}}\sum_{j\neq i\in\mathcal{I}} f_1(r||h_{ij}||_\sigma + ||p_{ij}||_\sigma)\frac{d}{dt}||p_{ij}||_\sigma \leq 0 \forall t \geq 0$. It is possible because f_1 is bounded and $|\frac{d}{dt}||p_{ij}||_\sigma| \leq \frac{1}{\sqrt{\epsilon}}||\dot{p}_{ij}||_2$, which converges exponentially fast. If algorithm (2) is applied, we have

$$\begin{aligned}
\dot{H}_1 &= \frac{1}{2}\sum_{i\in\mathcal{I}}\sum_{j\neq i\in\mathcal{I}} f_1(r||h_{ij}||_\sigma + ||p_{ij}||_\sigma)(r\frac{d}{dt}||h_{ij}||_\sigma + \frac{d}{dt}||p_{ij}||_\sigma) + \sum_{i\in\mathcal{I}} w_i\dot{w}_i + \dot{G} \\
&= \frac{1}{2}\sum_{i\in\mathcal{I}}\sum_{j\neq i\in\mathcal{I}} f_1(r||h_{ij}||_\sigma + ||p_{ij}||_\sigma)(r\frac{\partial||h_{ij}||_\sigma}{\partial z_i}\dot{z}_i + r\frac{\partial||h_{ij}||_\sigma}{\partial z_j}\dot{z}_j) \\
&\quad + \frac{1}{2}\sum_{i\in\mathcal{I}}\sum_{j\neq i\in\mathcal{I}} f_1(r||h_{ij}||_\sigma + ||p_{ij}||_\sigma)\frac{d}{dt}||p_{ij}||_\sigma + \sum_{i\in\mathcal{I}} w_i\dot{w}_i + \dot{G}
\end{aligned} \tag{4.10}$$

Since $\frac{\partial||h_{ij}||_\sigma}{\partial z_i} = \frac{\partial||h_{ij}||_\sigma}{\partial h_{ij}} = \hat{n}_{ij}$ and similarly $\frac{\partial||h_{ij}||_\sigma}{\partial z_j} = \hat{n}_{ji}$, so

$$\begin{aligned}
\dot{H}_1 &= \sum_{i\in\mathcal{I}} w_i \sum_{j\neq i\in\mathcal{I}} r f_1(r||h_{ij}||_\sigma + ||p_{ij}||_\sigma)\hat{n}_{ij} + \frac{1}{2}\sum_{i\in\mathcal{I}}\sum_{j\neq i\in\mathcal{I}} f_1(r||h_{ij}||_\sigma + ||p_{ij}||_\sigma)\frac{d}{dt}||p_{ij}||_\sigma \\
&\quad + \sum_{i\in\mathcal{I}} w_i\dot{w}_i + \dot{G} \\
&= \frac{1}{2}\sum_{i\in\mathcal{I}}\sum_{j\neq i\in\mathcal{I}} f_1(r||h_{ij}||_\sigma + ||p_{ij}||_\sigma)\frac{d}{dt}||p_{ij}||_\sigma - \sum_{i\in\mathcal{I}} k_w {w_i}^2 + \dot{G} \\
&\leq -\sum_{i\in\mathcal{I}} k_w {w_i}^2
\end{aligned} \tag{4.11}$$

For an non-autonomous system, the inequality above implies that the positive limit set for all solutions is included in the set where $w_i = 0 \ \ \forall i \in \mathcal{I}$. Furthermore, the vertical subsystem is asymptotically autonomous, then the positive limit set of all solutions is semi-invariant with respect to the system that the non-autonomous system converges to. Note that the semi-invariance is equivalent to invariance if the solution of the system is uniquely determined. Hence, we can conclude that all solutions of the system converge to the largest invariant set where $w_i = 0 \ \ \forall i \in \mathcal{I}$ with respect to the limiting system. In other words, all trajectories converge to the equilibriums of the limiting system, which are also the extremums $\lim_{t\to\infty} PE_1(z,t)$. It is assumed that all points but minimums of $\lim_{t\to\infty} PE_1(z,t)$ are unstable (this kind of assumption is made in [1], and is also used in [10, 12]). It can be observed that all minimums

of $\lim_{t\to\infty} PE_1(z,t)$ has the properties that $d_{ij}^{\sigma} \triangleq r||h_{ij}||_{\sigma} + ||p_{ij}||_{\sigma} \geq \hat{d}_{\sigma}$ between any two agents $i \neq j$, which concludes the statement. ■

4.2 Mode 2: Horizontal Separation

The basic objective for this mode of control protocol is to gain enough horizontal separations. In addition, it is required to avoid collisions without violating the constraint on the horizontal speed, assuming the control mode 1 has regulated the configuration of the system. The main techniques used in this part include the feedback linearizition and the artificial potential field method. The following definition is employed to the artificial potential field design for the control mode 2:

Definition 4.2.1 *$\psi_2 : \mathbb{R}^+ \mapsto \mathbb{R}^+$ is a candidate artificial potential function for control mode 2 if it has the following properties: (i) it is a monotone decreasing function with continuous derivative; and (ii) supp $\psi_2 = [0, \hat{d}_{\sigma}^{*}) \subsetneq [0, \hat{d}_{\sigma}) =$ supp ψ_1. The gradient of the candidate artificial potential function for control mode 2 is defined as*

$$f_2(\zeta) \triangleq \frac{d\psi_2(\eta)}{d\eta}|_{\eta=\zeta} \tag{4.12}$$

Besides the above definition, the next assumption introduces a constant that will be used for the design of control mode 2:

Assumption 1 *There is a constant K such that the following inequality is satisfied:*

$$K\psi_2(||d_{min}||_{\sigma}) > \sup_{||p_{ij}||_{\sigma} \geq ||d_{min}||_{\sigma}} \frac{1}{2} \sum_{i\in\mathcal{I}} \sum_{j\neq i\in\mathcal{I}} \psi_2(||p_{ij}||_{\sigma}), \tag{4.13}$$

where the supremum is taken over the cases where for any two agents $i \neq j$, $||p_{ij}||_{\sigma} \geq ||d_{min}||_{\sigma}$.

The constant K in the control protocol will be related to the ratio required between the control effort spent on collision avoidance and the control effort spent on the convergence. $\frac{N(N-1)}{2}$ can be a choice for K, but a smaller K could help to get less conservative result.

Feedback linearization technique is widely used for nonlinear system control design. Some related works applied this technique to simplify the problem (*e.g.*, [39]). The motivation of using this method is to convert the dynamics with nonholonomic constraint to the double integrator model, which makes the artificial potential field design more straightforward. The following coordinate transformation associates the horizontal accelerations of each agent with its control input for the horizontal motion:

$$\begin{bmatrix} u_{xi} \\ u_{yi} \end{bmatrix} \triangleq \begin{bmatrix} \ddot{x}_i \\ \ddot{y}_i \end{bmatrix} = \begin{bmatrix} \cos\theta_i & -\sin\theta_i \\ \sin\theta_i & \cos\theta_i \end{bmatrix} \begin{bmatrix} \dot{v}_i \\ v_i\dot{\theta}_i \end{bmatrix}. \tag{4.14}$$

Note that $v_i = 0$ is a singularity, but it is avoided if the constraint on the horizontal speed is not violated. For convenience, the vector $[\delta v_{xi}, \delta v_{yi}]^\intercal$ is defined as the following.

$$\begin{bmatrix} \delta v_{xi} \\ \delta v_{yi} \end{bmatrix} = \begin{bmatrix} v_{xi} - \hat{v}\cos\hat{\theta} \\ v_{yi} - \hat{v}\sin\hat{\theta} \end{bmatrix}, \tag{4.15}$$

where $v_R = [\hat{v}\cos\hat{\theta} \;\; \hat{v}\sin\hat{\theta}]^\intercal$ is the reference velocity whose magnitude $\hat{v}$ is in the open interval (v_{min}, v_{max}). It should be remarked that the constraint on the horizontal speed of each agent can be replaced with the constraint on $[\delta v_{xi}, \delta v_{yi}]^\intercal$.

The mode 2 of the control protocol in the new coordinate is given as

$$\begin{aligned} \begin{bmatrix} u_{xi} \\ u_{yi} \end{bmatrix} &= -\sum_{j\neq i} \Big\{ K f_2(r||h_{ij}||_\sigma + ||p_{ij}||_\sigma) + f_2(||p_{ij}||_\sigma) \Big\} \hat{\rho}_{ij} - \begin{bmatrix} k_x \delta v_{xi} \\ k_y \delta v_{yi} \end{bmatrix}, \\ \delta_i &= -\sum_{j\neq i} K r f_2(r||h_{ij}||_\sigma + ||p_{ij}||_\sigma) \hat{n}_{ij} - k_z w_i, \end{aligned} \tag{4.16}$$

where

$$\begin{aligned} \hat{\rho}_{ij} &\triangleq \frac{1}{\sqrt{1+\epsilon||p_{ij}||_2{}^2}} \begin{bmatrix} x_i - x_j \\ y_i - y_j \end{bmatrix}, \\ \hat{n}_{ij} &\triangleq \frac{h_{ij}}{\sqrt{1+\epsilon||h_{ij}||_2{}^2}}, \end{aligned} \tag{4.17}$$

and k_x, k_y and k_z are some positive constants; K is a constant that satisfies the inequality (4.13); f_2 is the gradient of a candidate artificial potential function for

control mode 2. It can be seen that each agent only requires the information from its horizontal neighbors. Strictly speaking, if two horizontally neighboring agents are vertically separated far away from each other, it might be difficult for these agents to obtain the required information from each other. However, it will not take place unless these agents are initially significantly separated in the vertical direction. Even if some agents are significantly separated in the vertical direction at the initial stage, some techniques in implementations could deal with it. For example, the original flocking group can be view as the collection of some subgroups in this case, then one can design an extra mode of control protocol to make these subgroups flies at approximately same altitude.

The main properties for the control mode 2 is summarized by the following theorem:

Theorem 4.2.1 *For the multi-agent system described by the equation (3.1) with Assumptions 1 hold, the following statements are true if the control (4.16) is applied:*

(I) $v_i(t) \in [v_{min}, v_{max}]$ $\forall t$ *if using appropriate* ψ_2, f_2 *and switching condition such that* $H_2(t_2) \triangleq \frac{1}{2}\sum_{i\in\mathcal{I}}\sum_{j\neq i\in\mathcal{I}}\left\{K\psi_2(r||h_{ij}||_\sigma+||p_{ij}||_\sigma)+\psi_2(||p_{ij}||_\sigma)\right\}+\frac{1}{2}\sum_{i\in\mathcal{I}}\left\{\delta {v_{xi}}^2+\delta {v_{yi}}^2+{w_i}^2\right\} \leq \frac{1}{2}\tilde{v}^2$, *where* $\tilde{v} \triangleq \min\{\hat{v}-v_{min}, v_{max}-\hat{v}\}$*;*

(II) There is no collision if for any two agents $i \neq j$, $||p_{ij}(t_2)||_\sigma \geq ||d_{min}||_\sigma$, $r||h_{ij}(t_2)||_\sigma+||p_{ij}(t_2)||_\sigma \geq \hat{d}^*_\sigma$ *and* $\frac{1}{2}\sum_{i\in\mathcal{I}}\left\{\delta v_{xi}(t_2)^2+\delta v_{yi}(t_2)^2+w_i(t_2)^2\right\} < \psi_2(||d_{min}||_\sigma)$*;*

(III) Almost every configuration the system approaches has the property that $||p_{ij}||_\sigma \geq \hat{d}^*_\sigma$ *for any two agents* $i \neq j$*;*

(IV) As $t \to \infty$, $v_i \to \hat{v}$, $\theta_i \to \hat{\theta}$, $w_i \to 0$ $\forall i \in \mathcal{I}$.

The first statement in the Theorem 4.2.1 is corresponding to the constraint on the horizontal speed. The second statement of the Theorem 4.2.1 is equivalent to say that there will not be any collision using the control mode 2 if the configuration of the system has been regulated by the control mode 1. The third statement claims that all agents will be separated in the horizontal direction. The last statement in the theorem declares that the heading angle, horizontal and vertical speeds of each agent will converge to the reference value.

The proof is still based on the artificial potential field method. A Hamiltonian function is defined as the sum of the total potential energy and the total kinetic energy, then it can be shown that the time derivative of this function is non-positive. If the initial Hamiltonian function value is small, then it will not get larger later, which implies that the constraint on the horizontal speed will be satisfied and collisions will be avoided. The statement related to the convergence properties can be shown using the standard LaSalle's invariance principle. The detailed proof is given as below.

Proof

Consider the Hamiltonian defined as below:

$$\begin{aligned} H_2 &\triangleq PE_2 + KE_2 \\ &\triangleq \frac{1}{2}\sum_{i\in\mathcal{I}}\sum_{j\neq i\in\mathcal{I}}\Big\{K\psi_2(r||h_{ij}||_\sigma + ||p_{ij}||_\sigma) + \psi_2(||p_{ij}||_\sigma)\Big\} + \frac{1}{2}\sum_{i\in\mathcal{I}}\Big\{\delta {v_{xi}}^2 + \delta {v_{yi}}^2 + {w_i}^2\Big\}, \end{aligned} \tag{4.18}$$

where K is the parameter introduced in Assumption 1 and used in the control (4.16). Note that H_2 is bounded below. If the control (4.16) is applied, we have

$$\begin{aligned} \dot{H}_2 = &\frac{1}{2}\sum_{i\in\mathcal{I}}\sum_{j\neq i\in\mathcal{I}}\Big\{Kf_2(r||h_{ij}||_\sigma + ||p_{ij}||_\sigma) + f_2(||p_{ij}||_\sigma)\Big\}\frac{d}{dt}||p_{ij}||_\sigma \\ &+ \frac{1}{2}\sum_{i\in\mathcal{I}}\sum_{j\neq i\in\mathcal{I}} Krf_2(r||h_{ij}||_\sigma + ||p_{ij}||_\sigma)\frac{d}{dt}||h_{ij}||_\sigma \\ &+ \sum_{i\in\mathcal{I}}\Big\{\delta v_{xi}u_{xi} + \delta v_{yi}u_{yi} + w_i\delta_i\Big\}. \end{aligned} \tag{4.19}$$

Recall that

$$\begin{aligned} \frac{d}{dt}||p_{ij}||_\sigma &= \nabla||p_{ij}||_\sigma^\intercal \dot{p}_{ij} \\ &= \frac{1}{\sqrt{1+\epsilon{||p_{ij}||_2}^2}}\{(x_i - x_j)(\dot{x}_i - \dot{x}_j) + (y_i - y_j)(\dot{y}_i - \dot{y}_j)\}, \end{aligned} \tag{4.20}$$

then

$$\begin{aligned}
&\frac{1}{2}\sum_{i\in\mathcal{I}}\sum_{j\neq i\in\mathcal{I}}\Big\{Kf_2(r||h_{ij}||_\sigma+||p_{ij}||_\sigma)+f_2(||p_{ij}||_\sigma)\Big\}\frac{d}{dt}||p_{ij}||_\sigma \\
&=\sum_{i\in\mathcal{I}}v_{xi}\sum_{j\neq i\in\mathcal{I}}\Big\{Kf_2(r||h_{ij}||_\sigma+||p_{ij}||_\sigma)+f_2(||p_{ij}||_\sigma)\Big\}\frac{x_i-x_j}{\sqrt{1+\epsilon||p_{ij}||_2{}^2}} \\
&\quad+\sum_{i\in\mathcal{I}}v_{yi}\sum_{j\neq i\in\mathcal{I}}\Big\{Kf_2(r||h_{ij}||_\sigma+||p_{ij}||_\sigma)+f_2(||p_{ij}||_\sigma)\Big\}\frac{y_i-y_j}{\sqrt{1+\epsilon||p_{ij}||_2{}^2}}.
\end{aligned} \tag{4.21}$$

Similarly,

$$\begin{aligned}
&\frac{1}{2}\sum_{i\in\mathcal{I}}\sum_{j\neq i\in\mathcal{I}}Krf_2(r||h_{ij}||_\sigma+||p_{ij}||_\sigma)\frac{d}{dt}||h_{ij}||_\sigma \\
&=\sum_{i\in\mathcal{I}}w_i\sum_{j\neq i\in\mathcal{I}}Krf_2(r||h_{ij}||_\sigma+||p_{ij}||_\sigma)\hat{n}_{ij}.
\end{aligned} \tag{4.22}$$

In addition,

$$\begin{aligned}
\sum_{i\in\mathcal{I}}\delta v_{xi}u_{xi}&=-\sum_{i\in\mathcal{I}}(v_{xi}-\hat{v}\cos\hat{\theta})\sum_{j\neq i}\Big\{Kf_2(r||h_{ij}||_\sigma+||p_{ij}||_\sigma)+f_2(||p_{ij}||_\sigma)\Big\}\frac{x_i-x_j}{\sqrt{1+\epsilon||p_{ij}||_2{}^2}} \\
&\quad-\sum_{i\in\mathcal{I}}k_x\delta v_{xi}{}^2 \\
&=-\sum_{i\in\mathcal{I}}v_{xi}\sum_{j\neq i}\Big\{Kf_2(r||h_{ij}||_\sigma+||p_{ij}||_\sigma)+f_2(||p_{ij}||_\sigma)\Big\}\frac{x_i-x_j}{\sqrt{1+\epsilon||p_{ij}||_2{}^2}} \\
&\quad-\sum_{i\in\mathcal{I}}k_x\delta v_{xi}{}^2,
\end{aligned} \tag{4.23}$$

where we have used $\hat{\rho}_{ij}=-\hat{\rho}_{ji}$. If we expand $\sum_{i\in\mathcal{I}}\delta v_{yi}u_{yi}$ and $\sum_{i\in\mathcal{I}}w_i\delta_i$in the same manner, we will get

$$\dot{H}_2=-\sum_{i\in\mathcal{I}}\Big\{k_x\delta v_{xi}{}^2+k_y\delta v_{yi}{}^2+k_z w_i{}^2\Big\}\leq 0 \tag{4.24}$$

To see (I), we consider the monotonicity: $H_2(t)\leq H_2(t_2)\forall t\geq t_2$. If $H_2(t_2)$ is small enough, the kinetic energy (the second term in H_2) will be limited. In detail, $\sqrt{\delta v_{xi}{}^2+\delta v_{yi}{}^2}\leq\tilde{v}\triangleq\min\{\hat{v}-v_{min},v_{max}-\hat{v}\}\forall t\geq t_2$ implies $v_i\in[v_{min},v_{max}]\forall t\geq t_1$. We can claim that if the control mode 2 is triggered when the inequality $H_2\leq\frac{1}{2}\tilde{v}^2$ is

satisfied, the velocity constraint can be guaranteed. It can be proved by contradiction: if it is not the case, there exists a t^* such that $H_2(t^*) > \frac{1}{2}\tilde{v}^2$ by the definition of H_2, but $H_2(t)$ is monotonically decreasing as shown before, which is contradictory to the assumption that the mode transition is triggered when the inequality $H_2 \leq \frac{1}{2}\tilde{v}^2$ is satisfied.

(II) can be proved by contradiction. First we assume two agents, say i and j, collide at $t = t^* \geq t_2$. That is $r||h_{ij}(t^*)||_\sigma + ||p_{ij}(t^*)||_\sigma \leq ||d_{min}||_\sigma$, which also implies $||p_{ij}(t^*)||_\sigma \leq ||d_{min}||_\sigma$. Hence

$$H_2(t^*) \geq \psi_2(||d_{min}||_\sigma) + K\psi_2(||d_{min}||_\sigma). \tag{4.25}$$

Since $||p_{ij}(t_2)||_\sigma \geq ||d_{min}||_\sigma$, $r||h_{ij}(t_2)||_\sigma + ||p_{ij}(t_2)||_\sigma \geq \hat{d}^*_\sigma$ and $\frac{1}{2}\sum_{i\in\mathcal{I}}\left\{\delta v_{xi}(t_2)^2 + \delta v_{yi}(t_2)^2 + w_i(t_2)^2\right\} < \psi_2(||d_{min}||_\sigma)$, we have

$$\begin{aligned} H_2(t_1) &< \sup_{||p_{ij}||_\sigma \geq ||d_{min}||_\sigma} \frac{1}{2}\sum_{i\in\mathcal{I}}\sum_{j\neq i\in\mathcal{I}} \psi_2(||p_{ij}||_\sigma) + \psi_2(||d_{min}||_\sigma) \\ &< K\psi_2(||d_{min}||_\sigma) + \psi_2(||d_{min}||_\sigma). \end{aligned} \tag{4.26}$$

However, $\dot{H}_2 \leq 0$ implies

$$H_2(t^*) \leq H_2(t_2) < \psi_2(||d_{min}||_\sigma) + K\psi_2(||d_{min}||_\sigma), \tag{4.27}$$

which is contradictory to (4.24).

(III) and (IV) can be shown by applying LaSalle's invariance principle. LaSalle's invariance principle states that all solutions to the system converge to the largest invariant set in the set where $\dot{H}_2$ is zero, which concludes (IV). The largest invariant set is nothing but the set of the equilibriums of the multi-agent system, which are also the extremums of PE_2. It is again assumed that all equilibriums but the minimums of PE_2 are unstable (the similar assumption is made in [1] and used in [10, 12]). Since the minimums of PE_2 has the property that $||p_{ij}||_\sigma \geq \hat{d}^*_\sigma$, we conclude the statement (III). It should be noticed that in practice, the unstable equilibriums can be simply excluded

by some implementation techniques. For example, since the unstable equilibriums are not corresponding to the global minimums of PE_2, one can perturb the configuration to make H_2 smaller, then by monotonicity of H_2, the unstable configuration can be excluded. ■

4.3 Mode 3: Horizontal Separation and Vertical Alignment

The control objective related to the final convergence properties, (O_3) and (O_4), will be achieved by using this control mode. In other words, each agent will gain the desired separation in the horizontal direction, and the altitude of each agent will converge to the same value. Meanwhile, the velocity constraint (O_1) and collision avoidance (O_2) are also addressed assuming the configuration of the multi-agent system has been regulated by the control mode 2.

It can be realized that all control objectives and constraints (O_1)-(O_4) are involved in this control mode. Although mode 3 of the control protocol will address all of these control objectives and constraints, the requirement on the initial state for this control mode is very restrictive, so the control mode 3 cannot be directly applied without the hybrid control structure. With the help of the control mode 1 and mode 2, the requirement on the initial state for the control mode 3 can be satisfied, which explains the necessity of the control mode 1 and mode 2 as well as the hybrid control structure of the proposed algorithm.

The basic methodologies for this mode of control include the artificial potential field method, feedback linearization and consensus algorithm for double-integrator dynamics. Similar to the system under the control mode 1, the dynamics under the control mode 3 can be decoupled into the horizontal subsystem and the vertical subsystem. The objective of the vertical subsystem is simply the consensus of the altitude, and the objective for the horizontal subsystem is to maintain the separation and address the velocity constraint and collision avoidance. The following definitions

are employed to the artificial potential field design and the adjacency function design for control mode 3.

Definition 4.3.1 *$\psi_3 : \mathbb{R}^+ \mapsto \mathbb{R}^+$ is a candidate artificial potential function for control mode 3 if it has the following properties: (i) it is a monotone decreasing function with continuous derivative; and (ii) supp $\psi_3 = [0, \hat{d}_\sigma^{**}) \subsetneq [0, \hat{d}_\sigma^{*}) =$ supp ψ_2. The gradient of the candidate artificial potential function for control mode 3 is defined as*

$$f_3(\zeta) \triangleq \frac{d\psi_3(\eta)}{d\eta}|_{\eta=\zeta} \tag{4.28}$$

Definition 4.3.2 *$adj : \mathbb{R}^+ \mapsto \mathbb{R}^+$ is a candidate adjacency function for the control mode 3 if it has the following properties: (i) it is a monotone decreasing function with continuous derivative; and (ii) supp $adj = [0, \hat{d}_\sigma^{**})$.*

With Definition 4.3.1, 4.3.2 and the feedback linearization (4.14), the mode 3 of the control protocol is proposed as

$$\begin{aligned} \begin{bmatrix} u_{xi} \\ u_{yi} \end{bmatrix} &= -\sum_{j\neq i} f_3(||p_{ij}||_\sigma)\hat{\rho}_{ij} - \begin{bmatrix} c_x \delta v_{xi} \\ c_y \delta v_{yi} \end{bmatrix}, \\ \delta_i &= -\sum_{j\neq i} adj(r||h_{ij}||_\sigma + ||p_{ij}||_\sigma)(w_i - w_j) - c_w w_i - c_z z_i, \end{aligned} \tag{4.29}$$

where $\hat{\rho}_{ij}$ has been defined in equation (4.17) and c_x, c_y, c_z, c_w are some positive constants; f_3 is the gradient of a candidate potential function for control mode 3; *adj* is a candidate adjacency function. Similar to the expression of control mode 2, the control for the horizontal motion subsystem is still based on the artificial potential method, so for each agent, the control only depends on the horizontally neighboring agents. For the vertical motion subsystem, the control is just a consensus algorithm for double integrator dynamics. Many existing works have investigated and extended the consensus algorithm for double integrator dynamics (*e.g.*, [21, 22, 55, 56]); the control used here can be replaced by other appropriate consensus algorithms, but without lose of generality, let us just consider this one for simplicity. Recall the assumption that the vertical distances between agents are not so large made in the

previous section. The same assumption is also appropriate here because the vertical distances between agents will converge to the same value. The main results for the controller mode 3 are summarized in the following theorem.

Theorem 4.3.1 *For the multi-agent system described by the equation (3.1), the following statements are true if the control (4.29) is applied:*

(I) $v_i(t) \in [v_{min}, v_{max}]$ $\forall t$ *if using appropriate* ψ_3, f_3 *and switching condition such that* $H_{3h}(t_3) \triangleq \frac{1}{2}\sum_{i\in\mathcal{I}}\sum_{j\neq i\in\mathcal{I}}\psi_3(||p_{ij}||_\sigma) + \frac{1}{2}\sum_{i\in\mathcal{I}}\left\{\delta v_{xi}{}^2 + \delta v_{yi}{}^2\right\} \leq \frac{1}{2}\tilde{v}^2$, *where* $\tilde{v} = \min\{\hat{v} - v_{min}, v_{max} - \hat{v}\}$;

(II) There is no collision if using appropriate ψ_3, f_3 *and switching condition such that* $H_{3h}(t_3) < \psi_3(||d_{min}||_\sigma)$;

(III) As $t \to \infty$, $v_i \to \hat{v}$, $\theta_i \to \hat{\theta}$, $w_i \to 0$, $z_i \to 0$ $\forall i \in \mathcal{I}$;

(IV) Almost every configuration that the system approaches has the property that for any two agents $i \neq j$, $||p_{ij}||_\sigma \geq \hat{d}^{**}_\sigma$;

The statements (I)-(IV) are exactly corresponding to the four global objectives (O_1)-(O_4). The proof for Theorem 4.3.1 is basically analogue to the proof of Theorem 4.2.1. Two Hamiltonian functions are defined for the horizontal subsystem and the vertical subsystem respectively. Then it can be shown that the time derivative of these two functions are non-positive. The statement (I) and (II) of Theorem 4.3.1 is the direct result from the monotonicity of the Hamiltonian functions. (III) and (IV) can be verified using LaSalle's invariance principle. The detailed proof is given as below.

Proof

Let us deal with the horizontal dynamics and vertical dynamics separately. For the horizontal dynamics, we consider the Hamiltonian defined as below:

$$H_{3h} = \frac{1}{2}\sum_{i\in\mathcal{I}}\sum_{j\neq i\in\mathcal{I}}\psi_3(||p_{ij}||_\sigma) + \frac{1}{2}\sum_{i\in\mathcal{I}}\left\{\delta v_{xi}{}^2 + \delta v_{yi}{}^2\right\}. \tag{4.30}$$

Thus,

$$\begin{aligned}\dot{H}_{3h} &= \frac{1}{2}\sum_{i\in\mathcal{I}}\sum_{j\neq i\in\mathcal{I}} f_3(||p_{ij}||_\sigma)\frac{d}{dt}||p_{ij}||_\sigma + \sum_{i\in\mathcal{I}}\Big\{\delta v_{xi}u_{xi} + \delta v_{yi}u_{yi}\Big\} \\ &= \sum_{i\in\mathcal{I}} v_{xi}\sum_{j\neq i\in\mathcal{I}} f_3(||p_{ij}||_\sigma)\frac{x_i - x_j}{\sqrt{1+\epsilon||p_{ij}||_2{}^2}} + \sum_{i\in\mathcal{I}} v_{yi}\sum_{j\neq i\in\mathcal{I}} f_3(||p_{ij}||_\sigma)\frac{y_i - y_j}{\sqrt{1+\epsilon||p_{ij}||_2{}^2}} \\ &\quad + \sum_{i\in\mathcal{I}}\Big\{\delta v_{xi}u_{xi} + \delta v_{yi}u_{yi}\Big\}.\end{aligned} \tag{4.31}$$

If the control (4.29) is applied, we have

$$\dot{H}_{3h} = -\sum_{i\in\mathcal{I}}\Big\{c_x\delta v_{xi}{}^2 + c_y\delta v_{yi}{}^2\Big\} \leq 0. \tag{4.32}$$

Similarly, for the vertical dynamics, we consider another Hamiltonian witch is defined as below:

$$H_{3v} = \frac{1}{2}\sum_{i\in\mathcal{I}} c_z z_i{}^2 + \frac{1}{2}\sum_{i\in\mathcal{I}} w_i{}^2. \tag{4.33}$$

Then

$$\dot{H}_{3v} = \sum_{i\in\mathcal{I}} c_z z_i w_i + \sum_{i\in\mathcal{I}} \delta_i w_i. \tag{4.34}$$

If the control (4.29) is applied, we have

$$\begin{aligned}\dot{H}_{3v} &= \sum_{i\in\mathcal{I}}\Big\{-c_w w_i{}^2 - w_i\sum_{j\neq i} adj(r||h_{ij}||_\sigma + ||p_{ij}||_\sigma)(w_i - w_j)\Big\} \\ &= -\sum_{i\in\mathcal{I}} c_w w_i{}^2 - \sum_{i\in\mathcal{I}}\sum_{j\neq i\in\mathcal{I}} adj(r||h_{ij}||_\sigma + ||p_{ij}||_\sigma)(w_i - w_j)^2 \\ &\leq 0.\end{aligned} \tag{4.35}$$

For (I), the monotonicity of H_{3h} implies that the velocity constraint can be satisfied if the initial energy is small, which can be realized by using appropriate ψ_3, f_3 and switching condition. The detailed proof is exactly same with the proof of the statement (I) of Theorem 4.2.1.

(II) can be shown, again using the monotonicity of H_{3h}: if initially the Hamiltonian is small enough, there will not be enough energy for collision later. Specifically, if $H_{3h}(t_3) < \psi_3(||d_{min}||_\sigma)$, there will not be any collision at any $t \geq t_3$. If it is not the

case, there exists $t^* \geq t_3$ such that $H_{3h}(t^*) \geq \psi_3(||d_{min}||_\sigma)$, which is contradictory to the fact that H_{3h} is monotonically decreasing.

(III) and (IV) can be proved by applying LaSalle's invariance principle: all solutions converge to the largest invariant set in the set where $\dot{H}_{3v} = \dot{H}_{3h} = 0$. The largest invariant set includes the equilibriums of the multi-agents system. Again we make the assumption that only the minimums of potential field are stable [1, 10, 12], then by the fact that the minimums of penitential field has the desired property, the proof is done. ■

4.4 Switching Logic Design

So far we have obtained three modes of control protocols, whose properties has been presented in Theorem 4.1.1, 4.2.1 and 4.3.1. In order to fulfill the global objectives and constraints (O_1)-(O_4) with relatively mild requirement on the initial state, the next problem is to determine a switching logic. We will first review the key properties of each control mode and then propose a switching logic based on that. For convenience, we define the subsets Ω_1, Ω_2, Ω_3 of the state space of the multi-agent system as

$$\begin{aligned}
&\Omega_1 : \mathcal{V} \cap \mathcal{A} \\
&\Omega_2 : \{H_2 \leq \frac{1}{2}\tilde{v}^2\} \cap \{H_2 < \psi_2(||d_{min}||_\sigma) + K\psi_2(||d_{min}||_\sigma)\} \\
&\Omega_3 : \{H_{3h} \leq \frac{1}{2}\tilde{v}^2\} \cap \{H_{3h} < \psi_3(||d_{min}||_\sigma)\}
\end{aligned} \tag{4.36}$$

where

$$\begin{aligned}
\mathcal{V} =& \Big\{ v_i \in [v_{min}, v_{max}], \quad \forall i \in \mathcal{I} \Big\} \\
\mathcal{A} =& \Big\{ ||p_{ij}||_2 - \{\frac{1}{k_v}|v_i - v_j| + \frac{\hat{v}}{k_\theta}|\theta_i - \theta_j| \\
&+ \frac{1}{k_v k_\theta}(\frac{v_i + v_j}{2} - \hat{v})|\theta_i - \theta_j|\} \geq d_{min}, \quad \forall i \neq j \in \mathcal{I} \Big\}
\end{aligned} \tag{4.37}$$

First, we see that if the multi-agent system starts from Ω_1 and the control mode 1 (4.2) is applied, the constraint on the horizontal velocity and collision avoidance will be satisfied, which has been verified by the statement (I) and (II) of Theorem 4.1.1.

In addition, for almost every initial state, the solution to the multi-agent system will converge to some subsets of Ω_2 as long as f_2 and ψ_2 are well-designed, which has been verified in the proof of statement (I), (III) of Theorem 4.1.1 and the statement (I), (II) of Theorem 4.2.1.

Then note that Ω_2 is a invariant set if the control mode 2 (4.16) is applied. Within Ω_2, the horizontal speed constraint and collision avoidance are automatically satisfied (see the statement (I) and (II) of Theorem 4.2.1). Furthermore, by the statement (III), (IV) of Theorem 4.2.1, almost every solution to the multi-agent system starting from Ω_2 converges to some subsets of Ω_3 as long as f_3 and ψ_3 are properly designed.

Similarly, Ω_3 is a invariant set if the control mode 3 (4.29) is applied. The horizontal speed constraint and collision avoidance are satisfied if the multi-agent system states are in Ω_3 by the statement (I), (II) of Theorem 4.3.1. Moreover, according to the statement (III) and (IV) of Theorem 4.3.1, the global objectives for convergence properties, (O_3) and (O_4), will be achieved.

Based on the above discussion, the following state-dependent logic for controller switch is one of the possible solution to achieve all control objectives with relatively mild requirement on the initial state (i.e. $x(t_0) \in \Omega_1 \cup \Omega_2 \cup \Omega_3$):

Algorithm 1: State-Dependent Logic for Controller Switch

```
Data: X_c = Multi-agent System State
Result: Controller Mode
if X_c ∈ Ω_3 then
    Controller Mode = 3 ;
else if X_c ∈ Ω_2 then
    Controller Mode = 2 ;
else
    Controller Mode = 1 ;
```

Fig. 4.3. State-Dependent Switching Logic

Equivalently, if $X_c \in \Omega_3$, the controller mode 3 is triggered; if $X_c \in \Omega_2 - \Omega_3$, the controller mode 2 is triggered; otherwise $X_c \in \mathcal{S} - \Omega_2 \cup \Omega_3$, the controller mode is assigned to be 1.

Remark 1 *Some works on the hybrid control may allow the infinitely fast mode change, for example, the sliding mode control. The infinitely fast mode change is impossible in practice, and the chattering of the controller could cause undesired behavior. The works that allow the fast mode change, in general, assume the behavior of the system with fast mode change can be approximately achieved by setting dwell time or other techniques. Nonetheless, considering the latency in supervisor-aircraft communication and the computation/communication capability of the supervisor for a large-scale system, it is not very practical to allow the supervisor to perform mode transition too frequently. The proposed switching logic is designed based on the invariance properties, so the frequent mode change can be avoided. It has been shown that Ω_2 and Ω_3 are invariant sets under the control mode 2 and 3 respectively, thus theoretically there are only finitely many mode changes, which significantly reduces the effect of asynchronization of mode transition between aircraft in practice.*

Remark 2 *It is totally fine to set a dwell time in the supervisor and (O_1)-(O_4) can still be guaranteed; in other words, the supervisor does not have to perform the algorithm too frequently and respond to aircraft immediately. It has been proved that there is a subset of Ω_2 that is invariant and attractive for almost every initial state under the control mode 1. It also has been proved that there is a subset of Ω_3 that is designed to be invariant and attractive for almost every initial state under the control mode 2. Due to these facts, whenever the supervisor performs the switching logic, the result is consistent; whenever the group of the aircraft receive the switching signal, the requirement on the initial state for the next control mode is always satisfied. Therefore, even if the supervisor does not perform the algorithm at every moment or there is latency in the supervisor-agent communication, all control objectives and constraints can still be satisfied.*

5. SIMULATION RESULTS

In this section, the simulation results will be presented. Specifically, Three cases corresponding to different initial conditions are simulated in the following sections. In addition, two extra algorithms that could possibly be considered are also simulated for comparative analysis. The main purpose of the comparative analysis is to illustrate that the switching control structure and the extra degree of freedom can indeed relax the requirement on the initial state.

The first control algorithm used for comparative analysis is nothing but only the mode 3 of the proposed hybrid flocking control algorithm. Recall that the mode 3 of the proposed algorithm can actually address all control objectives and constraints, but it induces a stronger requirement on the initial state. Note that the control mode 3 for the horizontal motion subsystem just follows the artificial potential field method, and the control mode 3 for vertical subsystem is just a consensus algorithm for double-integrator dynamics. Thus the control mode 3 can be treated as a simple extension of some previous works, *e.g.*, [1, 55]. We will show that the control mode 3 without hybrid control structure is not directly applicable in some cases because the required condition on the initial state can be too strong to be achieved.

The second control algorithm used for comparative analysis is similar to the proposed algorithm. It is also a multi-stage strategy, but we do not allow the vertical separation, *i.e.*, there are only the heading alignment stage and the control mode 3. The mode transition simply takes place when the headings and speeds are close to the desired value. This strategy could also be treated as a simple extension of some previous works, *e.g.*, [39]. The reason for considering this algorithm is to illustrate the effect of using the third degree of freedom during the transient stage. As mentioned in the main result, the use of the extra degree of freedom will relax the requirement on

the initial state. In the third simulation case, we will illustrate that the requirement is much stronger if the vertical motion is prohibited.

The parameters used in the simulation are summarized in the Table 5.1. Furthermore, the gradients of the artificial potential functions and the adjacency function used in the simulation are

$$
\begin{aligned}
f_1(d) &= \begin{cases} 10\tanh(0.025(d-12.5)) & , d \in [0, 12.5] \\ 0 & , d > 12.5 \end{cases}, \\
f_2(d) &= \begin{cases} 0.025\tanh(d-11) & , d \in [0, 11] \\ 0 & , d > 11 \end{cases}, \\
f_3(d) &= \begin{cases} 0.025\tanh(d-10.5) & , d \in [0, 10.5] \\ 0 & , d > 10.5 \end{cases}. \\
adj(d) &= \begin{cases} 1 & , d \in [0, 5.25] \\ 0.5(1+\cos(\pi(d/10.5-0.5)/0.5)) & , d \in [5.25, 10.5] \\ 0 & , d > 10.5 \end{cases}.
\end{aligned}
\tag{5.1}
$$

For the purpose of illustration, the constant K used in the mode 2 is simply $N(N-1)/2$. As mentioned before, the less conservative result can be obtained if a better approximation of K can be made.

Table 5.1.
Parameters Used in the Simulation

Parameters (for Objectives)	d_{min}	$\hat{d}$	r	ϵ
Value [Unit]	2 [m]	10 [m]	2	0.9
Parameters (for Objectives)	v_{min}	v_{max}	$\hat{v}$	$\hat{\theta}$
Value [Unit]	5 [m/s]	25 [m/s]	15 [m/s]	0 [rad]
Parameters (for Mode 1)	k_v	k_θ	k_w	
Value [Unit]	1 [1/s]	0.5 [1/s]	0.5 [1/s]	
Parameters for Mode 2	k_x	k_y	k_z	
Value [Unit]	0.1 [1/s]	0.1 [1/s]	0.5 [1/s]	
Parameters for Mode 3	c_x	c_y	c_z	c_w
Value [Unit]	0.1 [1/s]	0.1 [1/s]	0.1 [1/sˆ2]	0.5 [1/s]

5.1 Case I

The initial configuration for this case is basically randomly generated. Initially the agents are moderately separated in the horizontal direction but the velocity mismatch is large. The Figure 5.1 shows the initial pattern of agents. The plot of trajectories induced by the proposed algorithm is given in the Figure 5.2. Note that the different colors used in the trajectory plot stand for the different modes of control protocol during the process. Together with the Figure 5.3, one can conclude that there is no chattering.

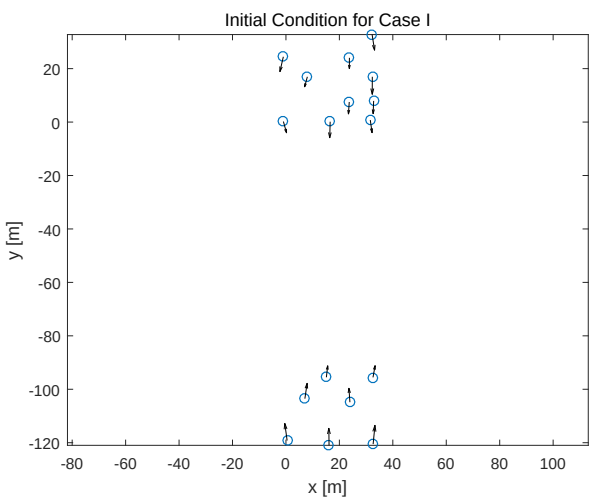

Fig. 5.1. Initial Configuration of Agents (for Case I)

The Figure 5.4 plots the time histories of the maximum and the minimum horizontal speeds among all agents. We can see that the horizontal speeds of all agents are bounded within the required interval. Collision avoidance and desire separations are achieved by using the proposed algorithm, which is shown in the Figure 5.5. In the same plot, we can also see that collision avoidance is not achieved using only the mode 3 of the control in this situation. It has been theoretically verified that the initial configuration of Case I satisfies the requirement of the proposed algorithm. However, the violation of collision avoidance implies that the initial configuration is

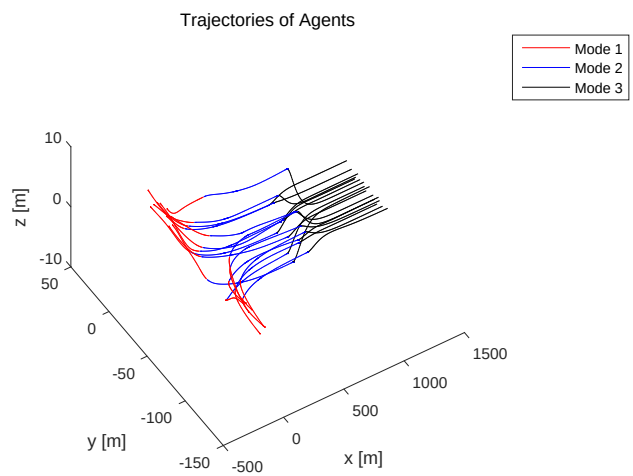

Fig. 5.2. Trajectories Induced by the Proposed Algorithm (for Case I)

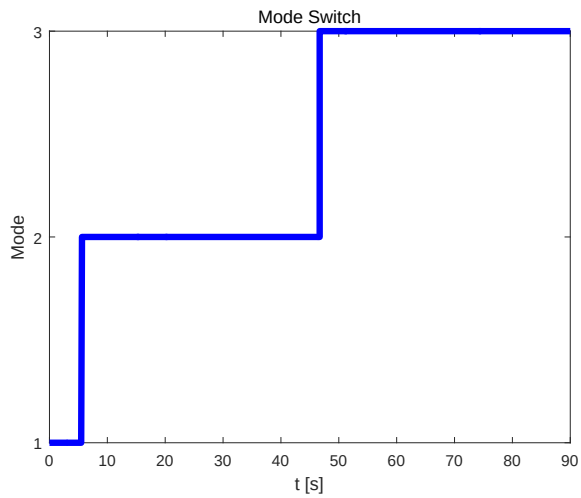

Fig. 5.3. Time History of the Mode Transition (for Case I)

not in the feasible set of the control mode 3. This explains the necessity of using the hybrid control structure.

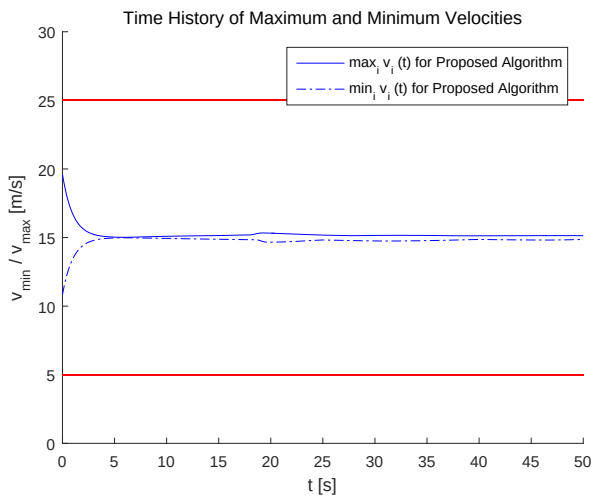

Fig. 5.4. Time Histories of the Maximum and the Minimum Horizontal Speeds Among All Agents (for Case I Using the Proposed Algorithm)

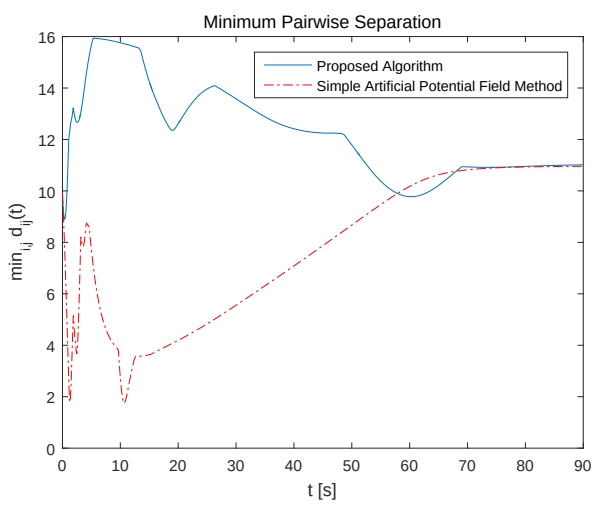

Fig. 5.5. The Minimum Separation Among All Pairs of Agents (for Case I)

5.2 Case II

The initial pattern of agents for Case II is presented in the Figure 5.6. In this case, all agents are very close to their neighbors, and in addition, the headings of agents are opposite to the desired direction though there is no velocity mismatch between agents. The proposed algorithm is able to achieve all objectives and constraints, which is shown in the Figure 5.7, 5.8 and 5.9. However, from the Figure 5.9, we can see that the constraint on the horizontal speed is not satisfied if only the mode 3 of the control is applied. It has been theoretically verified that the initial configuration of Case II satisfies the requirement of the proposed algorithm, but the violation of speed constraint implies that the initial configuration is not in the feasible set of the control mode 3. This also explains the necessity of using the hybrid control structure.

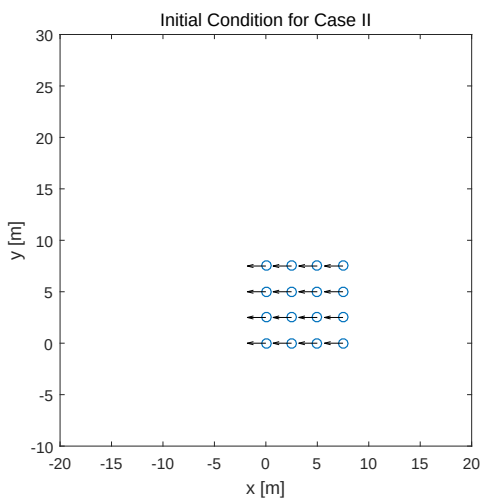

Fig. 5.6. Initial Configuration of Agents (for Case II)

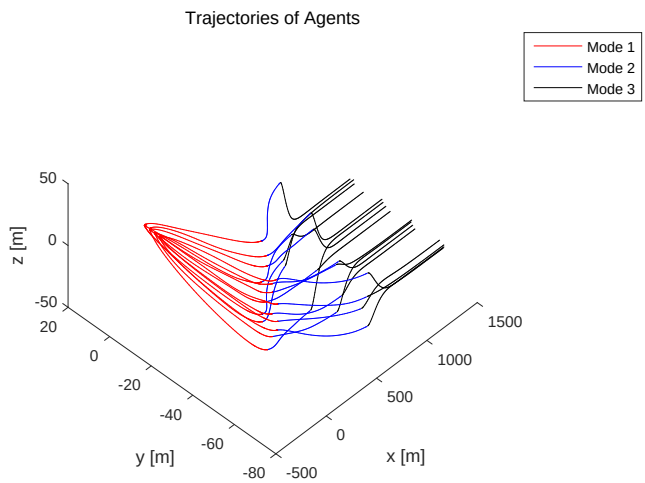

Fig. 5.7. Trajectories Induced by the Proposed Algorithm (for Case II)

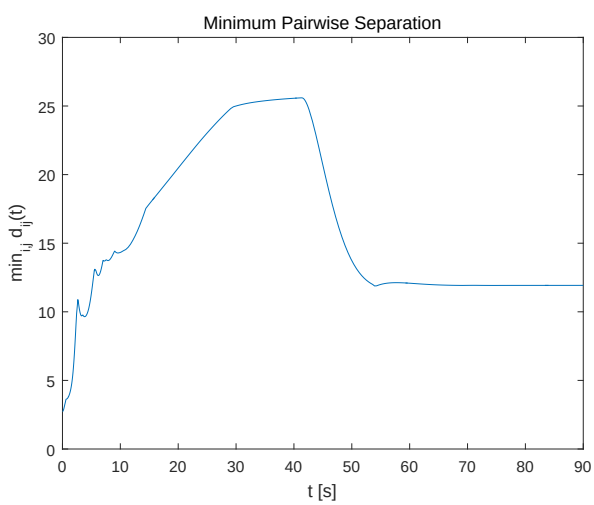

Fig. 5.8. The Minimum Separation Among All Pairs of Agents (for Case II Using the Proposed Algorithm)

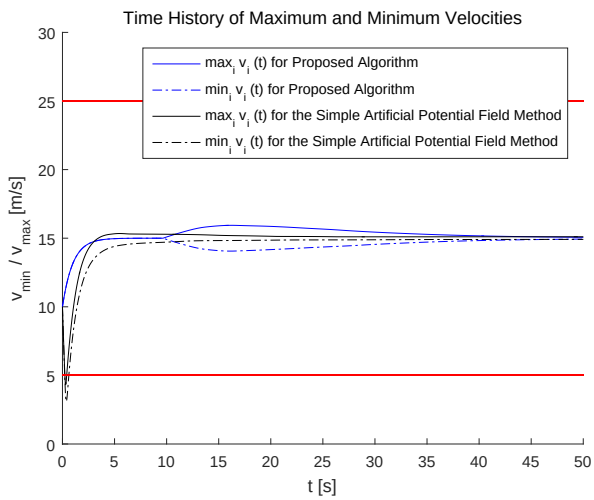

Fig. 5.9. Time Histories of the Maximum and the Minimum Horizontal Speeds Among All Agents (for Case II)

5.3 Case III

The initial configuration of agents for Case III is given in the Figure 5.10. This case is used to illustrate the necessity of the extra degree of freedom for collision avoidance. In this case, the proposed algorithm can fulfill all objectives and constraints, which can be concluded from the Figure 5.11, 5.12 and 5.13. However, the simple multi-stage control algorithm introduced at the beginning of this section cannot guarantee the collision avoidance, which can be concluded from the Figure 5.13. It can be theoretically verified that the initial configuration of Case III satisfies the requirement of the proposed algorithm, but the violation of collision avoidance implies that the initial configuration is not in the feasible set of initial states for the simple multi-stage control algorithm. This shows the necessity of using the third degree of freedom during the transient stage, also it explains how the efficient use of airspace is addressed by allowing the 3-D motion.

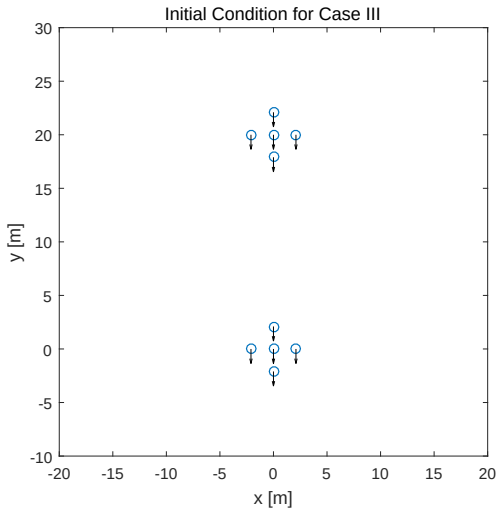

Fig. 5.10. Initial Configuration of Agents (for Case III)

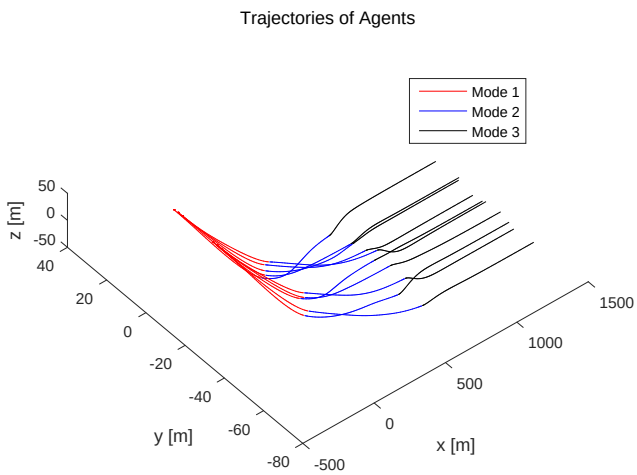

Fig. 5.11. Trajectories Induced by the Proposed Algorithm (for Case III)

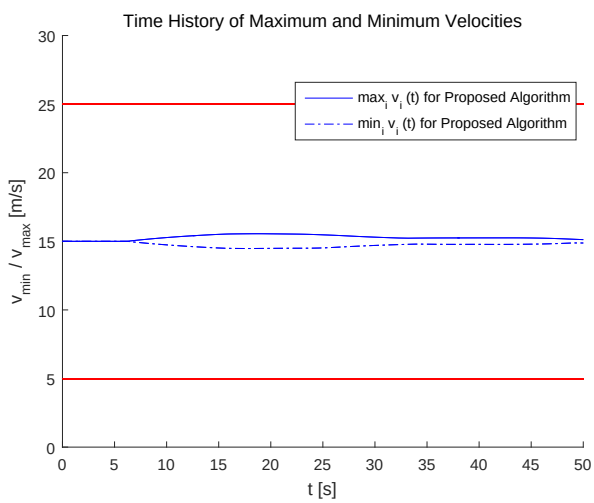

Fig. 5.12. Time Histories of the Maximum and the Minimum Horizontal Speeds Among All Agents (for Case III Using the Proposed Algorithm)

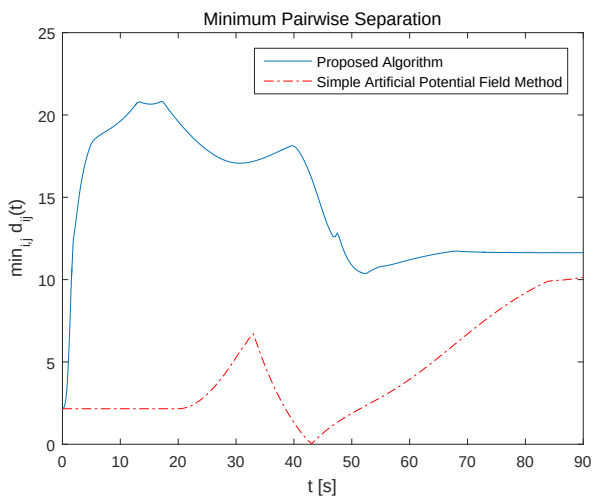

Fig. 5.13. The Minimum Separation Among All Pairs of Agents (for Case III)

6. CONCLUSION

This thesis has investigated the flocking control algorithm for a group of fixed-wing aircraft. Some practical concerns differentiate the fixed-wing aircraft flocking from general flocking problems, but none of the previous works have addressed these concerns simultaneously. In this work, a supervisory decentralized flocking control algorithm has been proposed to address the four practical concerns for fixed-wing aircraft flight, which include the nonholonomic constraint, the limitation of speed, collision avoidance and the efficient use of airspace. The proposed algorithm has been theoretically verified and numerically demonstrated.

In chapter 4, the main idea of the proposed flocking algorithm is presented in detail. To relax the requirement on the initial state, the proposed control algorithm has the switching control structure, which consists of three modes of control protocol and a state-dependent switching logic. The artificial potential field method has been applied to design the three modes of control protocol, and it has been proved that the nonholonomic constraint, the limitation of speed and collision avoidance can be addressed successfully. The state-dependent switching logic guarantees the desired convergence properties for flocking and addresses the efficient use of airspace. Since the switching logic is designed based on the invariance properties, the supervisor does not need to perform switchings frequently and respond to the agents immediately, which reveals that the presence of dwell time or delay will not prevent the algorithm from achieving the objectives.

In chapter 5, the simulation results of three different flocking scenarios are presented to illustrate the effect of using the extra degree of freedom and the switching control structure. In the first two cases, the proposed algorithm is compared with the algorithm that only consists of the control mode 3 of the proposed algorithm. The simulation results show that for the first two cases, all objectives and constraints can

be achieved by the proposed algorithm with the switched control structure, but either the limitations of speed or collision avoidance fails if only the control mode 3 without the hybrid control structure is applied. In the third case, the proposed algorithm is compared with another algorithm that consists of the control mode 1 and 3 with only the 2-dimensional motion allowed. The simulation results show that for the third case, all of the objectives and constraints can be fulfilled by the proposed algorithm, but collision avoidance is violated if the 3-dimensional motion is not allowed.

The main contribution of the proposed algorithm is to addresses all aforementioned concerns simultaneously without too restrictive conditions on the initial state. For the future extension of the research, the possible directions include: (i) addressing flocking centering in an effective way based on the proposed framework; (ii) considering more performance indexes for the algorithm, for examples, the convergence rate, the capability to reject the disturbance; and (iii) investigating the decentralized schemes to perform the switching logic.

REFERENCES

REFERENCES

[1] R. Olfati-Saber, "Flocking for multi-agent dynamic systems: Algorithms and theory," *IEEE Trans. Autom. Control*, vol. 51, no. 3, pp. 401–420, Mar. 2006.

[2] A. Jadbabaie, J. Lin, and A. S. Morse, "Coordination of groups of mobile autonomous agents using nearest neighbor rules," *IEEE Trans. Autom. Control*, vol. 48, no. 6, pp. 988–1001, Jun. 2003.

[3] V. Gazi and K. M. Passino, "Stability analysis of swarms," *IEEE Trans. Autom. Control*, vol. 48, no. 4, pp. 692–697, 2003.

[4] H. G. Tanner, A. Jadbabaie, and G. J. Pappas, "Stable flocking of mobile agents, part i: Fixed topology," in *Proc. 42nd IEEE Conf. Decision and Control*, Dec. 2003, pp. 2010–2015.

[5] ——, "Stable flocking of mobile agents, part ii: Dynamic topology," in *Proc. 42nd IEEE Conf. Decision and Control*, Dec. 2003, pp. 2016–2021.

[6] T. Vicsek, A. Czirok, E. Ben-Jacob, I. Cohen, and O. Shochet, "Novel type of phase transition in a system of self-driven particles," *Phys. Rev. Lett.*, vol. 75, no. 6, pp. 1226–1229, Aug. 1995.

[7] C. W. Reynolds, "Flocks, herds, and schools: A distributed behavioral model," in *Comput. Graph. (ACM SIGGRAPH87 Conf. Proc.)*, Jul. 1987, pp. 25–34.

[8] Z. Chen, H.-T. Zhang, M.-C. Fan, D. Wang, and D. Li, "Algorithms and experiments on flocking of multiagents in a bounded space," *IEEE Trans. Control Syst. Technol.*, vol. 22, no. 4, pp. 1544–1549, Jul. 2014.

[9] W. Li, "Unified generic geometric-decompositions for consensus or flocking systems of cooperative agents and fast recalculations of decomposed subsystems under topology-adjustments," *IEEE Trans. Cybern.*, vol. 46, no. 6, pp. 1463–1470, Jun. 2016.

[10] H. Su, X. Wang, and Z. Lin, "Flocking of multi-agents with a virtual leader," *IEEE Trans. Autom. Control*, vol. 54, no. 2, pp. 293–307, Feb. 2009.

[11] Z. Chen, M.-C. Fan, and H.-T. Zhang, "How much control is enough for network connectivity preservation and collision avoidance?" *IEEE Trans. Cybern.*, vol. 45, no. 8, pp. 1647–1656, Aug. 2015.

[12] H. Su, X. Wang, and G. Chen, "A connectivity-preserving flocking algorithm for multi-agent systems based only on position measurements," *Int. J. Control*, vol. 82, no. 7, pp. 1334–1343, Jul. 2009.

[13] M. Ji and M. Egerstedt, "Distributed coordination control of multiagent systems while preserving connectedness," *IEEE Trans. Robot.*, vol. 23, no. 4, pp. 693–703, Aug. 2007.

[14] J. Zhan and X. Li, "Flocking of multi-agent systems via model predictive control based on position-only measurements," *Trans. Ind. Informat.*, vol. 9, no. 1, pp. 377–385, Feb. 2013.

[15] G. Ferrari-Trecate, L. Galbusera, M. P. E. Marciandi, and R. Scattolini, "Model predictive control schemes for consensus in multi-agent systems with single- and double-integrator dynamics," *IEEE Trans. Autom. Control*, vol. 54, no. 11, pp. 2560–2572, Feb. 2009.

[16] A. Ulusoy, O. Gurbuz, and A. Onat, "Wireless model-based predictive networked control system over cooperative wireless network," *Trans. Ind. Informat.*, vol. 7, no. 1, pp. 41–51, Feb. 2011.

[17] J. Zhan and X. Li, "Decentralized flocking protocol of multi-agent systems with predictive mechanisms," in *Proc. 30th China Control Conf.*, Jul. 2011, pp. 5995–6000.

[18] H.-T. Zhang, M. Z. Chen, G.-B. Stan, T. Zhou, and J. M. Maciejowski, "Collective behavior coordination with predictive mechanisms," *IEEE Circuits Syst. Mag.*, vol. 8, no. 3, pp. 67–85, 2008.

[19] A. Ajorlou, A. Momeni, and A. G. Aghdam, "A class of bounded distributed control strategies for connectivity preservation in multi-agent systems," *IEEE Trans. Autom. Control*, vol. 55, no. 12, pp. 2828–2833, Dec. 2010.

[20] R. Olfati-Saber, J. A. Fax, and R. M. Murray, "Consensus and cooperation in networked multi-agent systems," *Proc. of the IEEE*, vol. 95, no. 1, pp. 215–233, Jan. 2007.

[21] W. Ren, "On consensus algorithms for double-integrator dynamics," *IEEE Trans. Autom. Control*, vol. 53, no. 6, pp. 1503–1509, Jul. 2008.

[22] A. Abdessameud and A. Tayebi, "On consensus algorithms design for double integrator dynamics," *Automatica*, vol. 49, no. 1, pp. 253–260, 2013.

[23] J. A. Gouvea, F. Lizarralde, and L. Hsu, "Potential function formation control of nonholonomic mobile robots with curvature constraints," in *Proc. 18th World Congr. IFAC*, 2011, pp. 11 931–11 936.

[24] B. Lei, W. Li, and F. Zhang, "Flocking algorithm for multi-robots formation control with a target steering agent," in *Proc. 2008 IEEE Int. Conf. System, Man and Cybernetics*, 2008, pp. 3536–3541.

[25] Q. Li and Z.-P. Jiang, "Flocking control of multiagent systems with application to nonholonomic multirobots," *KYBERNETIKA*, vol. 45, no. 1, pp. 84–100, 2009.

[26] M. Jafarian, "Ternary and hybrid controllers for the rendezvous of unicycles," in *Proc. 2015 IEEE 54th Conf. Decision and Control*, 2015, pp. 2353–2358.

[27] X.-W. Zhao, B. Hu, Z.-H. Guan, C.-Y. Chen, M. Chi, and X.-H. Zhang, "Multi-flocking of networked non-holonomic mobile robots with proximity graphs," *IET Control Theory & Applications*, vol. 10, no. 16, pp. 2093–2099, 2016.

[28] Y. Liang and H.-H. Lee, "Decentralized formation control and obstacle avoidance for multiple robots with nonholonomic constraints," in *Proc. 2006 American Control Conf.*, 2006, pp. 5596–5601.

[29] K. D. Do, "Formation tracking control of unicycle-type mobile robots with limited sensing ranges," *IEEE Trans. Control Syst. Technol.*, vol. 16, no. 3, pp. 527–538, May. 2008.

[30] A. Ajorlou and A. G. Aghdam, "Connectivity preservation in nonholonomic multi-agent systems: A bounded distributed control strategy," *IEEE Trans. Autom. Control*, vol. 58, no. 9, pp. 2366–2371, Sep. 2013.

[31] S. Mastellone, D. M. Stipanovic, C. R. Graunke, K. A. Intlekofer, and M. Spong, "Formation control and collision avoidance for multi-agent non-holonomic systems: Theory and experiments," *Int. J. Robot. Research*, vol. 27, no. 1, pp. 107–126, Jan. 2008.

[32] K. Cao, B. Jiang, and D. Yue, "Distributed consensus of multiple nonholonomic mobile robots," *IEEE/CAA J. Automatica Sinica*, vol. 1, no. 2, pp. 162–170, Apr. 2014.

[33] K. D. Listmann, M. V. Masalawala, and J. Adamy, "Consensus for formation control of nonholonomic mobile robots," in *Proc. 2009 IEEE Int. Conf. Robotics and Automation*, 2009, pp. 3886–3891.

[34] J. Jin, Y.-G. Kim, S.-G. Wee, and N. Gans, "Consensus based attractive vector approach for formation control of nonholonomic mobile robots," in *Proc. 2015 IEEE Int. Conf. Advanced Intelligent Mechatronics*, 2015, pp. 977–983.

[35] Z. Qu, J. Wang, and R. A. Hull, "Cooperative control of dynamical systems with application to autonomous vehicles," *IEEE Trans. Autom. Control*, vol. 53, no. 4, pp. 894–911, May 2008.

[36] M. Abouheaf and W. Gueaieb, "Flocking motion control for a system of nonholonomic vehicles," in *Proc. 2017 IEEE Int. Symp. Robotics and Intelligent Sensors*, 2017, pp. 32–37.

[37] W. Dong and J. A. Farrell, "Cooperative control of multiple nonholonomic mobile agents," *IEEE Trans. Autom. Control*, vol. 53, no. 6, pp. 1434–1448, Jul. 2008.

[38] X.-W. Zhao, Z.-H. Guan, J. Li, X.-H. Zhang, and C.-Y. Chen, "Flocking of multi-agent nonholonomic systems with unknown leader dynamics and relative measurements," *Int. J. Robust Nonlinear Control*, vol. 27, no. 17, pp. 3685–3702, 2017.

[39] T. Liu and Z.-P. Jiang, "Distributed formation control of nonholonomic mobile robots without global position measurements," *Automatica*, vol. 49, no. 2, pp. 592–600, 2013.

[40] X. Zhang and H. Duan, "Altitude consensus based 3d flocking control for fixed-wing unmanned aerial vehicle swarm trajectory tracking," *Proceedings of the Institution of Mechanical Engineers, Part G: Journal of Aerospace Engineering*, vol. 230, no. 14, pp. 2628–2638, 2016.

[41] X.-W. Zhao, M. Chi, Z.-H. Guan, B. Hu, and X.-H. Zhang, "Flocking of multiple three-dimensional nonholonomic agents with proximity graph," *Journal of the Franklin Institute*, vol. 354, no. 8, pp. 3617–3633, 2017.

[42] J. Zhu, J. L, and X. Yu, "Flocking of multi-agent non-holonomic systems with proximity graphs," *IEEE Trans. Circuits Syst. I, Reg. Papers*, vol. 60, no. 1, pp. 199–210, Jan. 2013.

[43] N. Moshtagh and A. Jadbabaie, "Distributed geodesic control laws for flocking of nonholonomic agents," *IEEE Trans. Autom. Control*, vol. 52, no. 4, pp. 681–686, Apr. 2007.

[44] N. Moshtagh, N. Michael, A. Jadbabaie, and K. Daniilidis, "Vision-based, distributed control laws for motion coordination of nonholonomic robots," *IEEE Trans. Robot.*, vol. 25, no. 4, pp. 851–860, Aug. 2009.

[45] R. Sepulchre, D. A. Paley, and N. E. Leonard, "Stabilization of planar collective motion: All-to-all communication," *IEEE Trans. Autom. Control*, vol. 52, no. 5, pp. 811–824, May. 2007.

[46] C. Kownacki and D. Oldziej, "Fixed-wing uavs flock control through cohesion and repulsion behaviours combined with a leadership," *International Journal of Advanced Robotic Systems*, vol. 13, no. 1, p. 36, 2016.

[47] S. Bayraktar, G. E. Fainekos, and G. J. Pappas, "Experimental cooperative control of fixed-wing unmanned aerial vehicles," in *Proc. 43rd IEEE Conf. Decision and Control*, 2004, pp. 4292–4298.

[48] T. H. Chung, M. R. Clement, M. A. Day, K. D. Jones, D. Davis, and M. Jones, "Live-fly, large-scale field experimentation for large numbers of fixed-wing uavs," in *Proc. 2016 IEEE Int. Conf. Robotics and Automation*, 2016, pp. 1255–1262.

[49] L. Perea, G. Gmez, and P. Elosegui, "Extension of the cuckersmale control law to space flight formations," *Journal of Guidance, Control, and Dynamics*, vol. 32, no. 2, pp. 526–536, 2009.

[50] D. J. Bennet, C. R. McInnes, M. Suzuki, and K. Uchiyama, "Autonomous three-dimensional formation flight for a swarm of unmanned aerial vehicles," *Journal of Guidance, Control, and Dynamics*, vol. 34, no. 6, pp. 1899–1908, 2011.

[51] E. W. Justh and P. S. Krishnaprasad, "Steering laws and continuum models for planar formations," in *42nd IEEE Conf. Decision and Control*, vol. 4, 2003, pp. 3609–3614.

[52] a. D. Z. Jiafu Wan, S. Zhao, L. Yang, and J. Lloret, "Context-aware vehicular cyber-physical systems with cloud support: architecture, challenges, and solutions," *IEEE Communications Magazine*, vol. 52, no. 8, pp. 106–113, 2014.

[53] M. C. Consiglio, J. P. Chamberlain, C. A. Munoz, and K. D. Hoffler, "Concepts of integration for uas operations in the nas," 2012.

[54] N. Rouche, P. Habets, and M. Laloy, *Stability theory by Liapunov's direct method.* Springer, 1977, vol. 4.

[55] W. Ren, "Consensus strategies for cooperative control of vehicle formations," *IET Control Theory & Applications*, vol. 1, no. 2, pp. 505–512, 2007.

[56] W. Ren and E. Atkins, "Distributed multi-vehicle coordinated control via local information exchange," *International Journal of Robust and Nonlinear Control*, vol. 17, no. 10-11, pp. 1002–1033, 2007.

[57] A. Zvi, "Appendix a: Limiting equations and stability of nonautonomous ordinary differential equations," in *The Stability of Dynamical Systems.* SIAM, 1976, pp. 57–76.